Atmos. Chem. Phys., 26, 16779–16803, 2026
https://doi.org/10.5194/acp-26-16779-2026
© Author(s) 2026. This work is distributed under
the Creative Commons Attribution 4.0 License.

Atmospheric Chemistry and Physics
Open Access
EGU

New processes to counteract sedimentation of coarse dust particles are required for climate models to agree with aircraft observations

Natalie G. Ratcliffe[1,a], Claire L. Ryder[1], Nicolas Bellouin[1], Anthony Jones[2], Ben Johnson[2], Stephanie Woodward[2], Lisa-Maria Wieland[3], Josef Gasteiger[3,b], and Bernadett Weinzierl[3]

[1]Department of Meteorology, University of Reading, Reading, UK
[2]Met Office Hadley Centre, Exeter, UK
[3]Faculty of Physics, Aerosol Physics and Environmental Physics, University of Vienna, Boltzmanngasse 5, 1090 Vienna, Austria
[a]now at: Atmospheric, Oceanic and Planetary Physics, University of Oxford, Oxford, UK
[b]now at: Hamtec Consulting GmbH at EUMETSAT, Darmstadt, Germany

Correspondence: Natalie G. Ratcliffe (natalie.ratcliffe@physics.ox.ac.uk)

Received: 16 October 2025 – Discussion started: 5 November 2025
Revised: 16 November 2026 – Accepted: 17 November 2026 – Published: 24 November 2026

Abstract. Recent observations reveal coarse (diameter $> 2.5\,\mu m$) mineral dust particles are transported unexpectedly great distances from their Saharan source. Transport models represent this coarse dust transport poorly, having important feedbacks on Earth's radiative budget, carbon and hydrological cycles, and human health. We carry out sensitivity tests on the trans-Atlantic transport and deposition processes governing the long-range evolution of mineral dust size distribution in a climate model (HadGEM3-GA7.1). We test the sensitivity of coarse particle transport (up to 63.2 µm diameter) to sedimentation, convective and turbulent mixing, impaction scavenging, and dust shortwave absorption by removing or scaling the magnitude of these processes. Reductions in sedimentation velocity of 50 %–95 % bring modelled coarse particle transport into better agreement with in-situ aircraft observations with the required reduction increasing with transport distance. Other tested processes do not result in the multiple order of magnitude changes in transported dust mass required for agreement with observations. We infer that additional process/es which are misrepresented or missing in the model must be acting to counteract particle sedimentation. Convective and turbulent mixing have minimal impact on coarse particle transport in the model but are key in controlling the vertical distribution of dust in the Saharan air layer and marine boundary layer. Impaction scavenging dominantly impacts fine dust concentration. This study adds to the growing body of evidence pointing to processes involved in coarse mineral dust transport and deposition which are not represented accurately or at all in models, which counteract the sedimentation of coarse particles in the real-world.

1 Introduction

As the most abundant natural aerosol in the atmosphere by mass, mineral dust has wide-ranging impacts on the Earth system and human activities. Impacting climate, weather, ecosystems (e.g. Kok et al., 2023; Shao et al., 2011), and anthropogenic activities, through altering Earth's radiative budget, carbon and hydrological cycles, human health, aviation, air quality and solar energy. Dust particle size influences the magnitude of these impacts. Fine (diameter $(d) < 2.5\,\mu m$), coarse ($2.5 < d < 10\,\mu m$), super-coarse ($10 < d < 62.5\,\mu m$), and giant ($d > 62.5\,\mu m$) (size ranges as defined by Adebiyi et al., 2023) particles vary in terms of mass, mineralogical composition, solubility, and morphology, affecting their interactions with radiation (Adebiyi and Kok, 2020; Adebiyi et al., 2023; Tegen and Lacis, 1996), their impact on bio-

geochemistry (Marcotte et al., 2020), their efficacy as cloud condensation nuclei (Karydis et al., 2011) and ice nucleating particles (Adebiyi et al., 2023), and their interactions with the human body (Kotsyfakis et al., 2019). Henceforth, particles with $d > 2.5\,\mu m$ (i.e. coarse, super-coarse, and giant particles) will be referred to collectively as coarse particles for simplicity, though where appropriate, the individual size ranges will be specified. Coarse particles have been assumed to have relatively short, or even negligible, atmospheric lifetimes based on their larger diameter, and hence mass and calculated Stokes setting velocity. In theory, a spherical dust particle of $d = 30\,\mu m$ at 5 km altitude in the Saharan atmospheric boundary layer (SABL) should be deposited to the surface in ~ 20 h (Ryder et al., 2013a). Therefore, due to the assumed short lifetime, and sampling constraints associated with instrument inlets and pipework (Rosenberg et al., 2014; Ryder et al., 2019), coarse particles were not typically measured in observational campaigns. They are also often disregarded in global climate models (GCMs) for this same reason and the additional computational expense, resulting in most models not representing particles greater than 10 or 20 µm in diameter (Gliß et al., 2021; Zhao et al., 2022). Some observational measurements recorded long-range transport of coarse particles over hundreds or thousands of kilometres further than expected (e.g. Betzer et al., 1988), but it was not until the last 20 years that new research became focused on measuring these particles and understanding the quantity and size distribution of coarse particles in the atmosphere (Ryder et al., 2013b, a, 2018, 2019; van der Does et al., 2016, 2018; Varga et al., 2021; Weinzierl et al., 2009, 2017).

The discovery of longer-range transport of coarse particles has triggered research exploring how these particles are retained in the Earth's atmosphere and the consequent impacts of a greater atmospheric mass loading than previously thought. With a larger coarse particle presence, the top-of-atmosphere (TOA) shortwave (SW) effect of dust is less cooling and the TOA longwave (LW) effect is more warming than previously estimated (Adebiyi and Kok, 2020). This results in a total direct radiative effect (DRE) of all dust being less cooling than previously thought at approximately $-0.15 \pm 0.35\,W\,m^{-2}$ (Kok et al., 2023). This value remains uncertain partly due to poor understanding of the quantity and lifetime of coarse dust particles in the atmosphere. Kok et al. (2026) estimated that climate models underestimate the LW DRE of dust by 50 % due to misrepresentations of coarse particle load and their radiative effects in the atmosphere.

Despite recent advances in our understanding of the coarse size distribution of mineral dust in our atmosphere over long-range transport, climate and forecast models continue to underestimate coarse particle loading and transport (Adebiyi and Kok, 2020). Ryder et al. (2019) found that at least 40 % of the dust mass lofted at the Sahara was greater than 20 µm in diameter, suggesting models with size cut-off at 10–20 µm will strongly underestimate atmospheric dust mass. Additionally, many models also tune dust emissions so that the magnitude and distribution of total dust aerosol optical depth (AOD) agrees with satellite or ground-based retrievals of AOD (O'Sullivan et al., 2020). However, since AOD is most sensitive to the fine dust size range, coarse dust remains unconstrained and fine dust may be overrepresented. If a model experiences such imbalances in microphysical processes, the tuning towards observed AOD alone may result in the model having to compensate for these imbalances by altering the intensity of aerosol sources and sinks (O'Sullivan et al., 2020). As a result of AOD tuning and lack of or underrepresentation of coarse particles, a bias towards fine dust particles is created which is evident in many models (Evan et al., 2014; Kok, 2011; Kok et al., 2017; Ratcliffe et al., 2024), resulting in significant dust mass underestimations both at emission and during transport. This also results in underestimations of deposited dust mass downstream (Checa-Garcia et al., 2021).

The AeroCom (Aerosol Comparisons between Observations and Models) Phase III initiative found that since AeroCom Phase I, recent iterations of climate models are more likely to represent coarse dust particles, but that the models generally still show a fine size bias (Gliß et al., 2021). The Met Office Unified Model (MetUM; from which the HadGEM3-GA7.1 model configuration used in this paper originates) represents dust particles in six size bins up to 63.2 µm diameter. However, Ratcliffe et al. (2024) showed that while these coarse particles are emitted in the model, they are deposited too rapidly relative to aircraft observations, resulting in an increasing fine size bias with distance from the source. Specifically, they found that between 2–3.7 km altitude at the Sahara, HadGEM3-GA7.1 underestimated dust mass contribution of 20–63.2 µm diameter particles to total mass by ~ 40 %, consistent with the value suggested by Ryder et al. (2019). The model underestimate increased with transport as the coarse particles were more swiftly deposited in the model than the observations. Upon transport to the Caribbean, there was a negligible mass of 20–63.2 µm particles remaining in the model but observations confirmed the presence of these particles as they still made up ~ 10 % of the total dust mass observed. They also showed that while the total dust mass was transported at the correct altitude, the coarse dust mass was transported too low in the atmosphere. This corroborated the findings of O'Sullivan et al. (2020), who found that in a numerical weather prediction (NWP) version of the MetUM, with a more simple dust scheme in two size bins up to 20 µm diameter, and in the European Centre for Medium-Range Weather Forecasts (ECMWF) Copernicus Atmosphere Monitoring Service (CAMS) forecast model, the coarse dust was also transported too low in the atmosphere.

The mechanisms and processes which have been postulated to drive the unexplained retention of coarse dust during long-range transport are as follows:

Asphericity: Dust particles are typically modelled as spheres, though in reality they tend to be much more aspherical (Huang et al., 2020; Otto et al., 2011). Aspherical particles experience enhanced drag, increasing particle transport altitude (Colarco et al., 2014; Yang et al., 2013) and lifetime (Mallios et al., 2020; Saxby et al., 2018), Huang et al. (2020) estimate an increase in coarse particle lifetime by $\sim 20\,\%$. If the particles were oriented horizontally (with its longest axis parallel to the surface) in the atmosphere, the increase in drag and lifetime would be even greater (Mallios et al., 2020).

Electric charging: Dust particles can undergo charging through collisions with other dust particles (triboelectrification), leading to the whole dust plume carrying observable charge (Harrison et al., 2018; Nicoll et al., 2011, 2020; Savvakis et al., 2024). Charged particles may be able to travel higher in the atmosphere with longer lifetime (Méndez Harper et al., 2022) as a result of their interaction with the Earth's electric field, and have been shown to be transported higher than non-charged particles in a laboratory setting (Toth et al., 2020). In-situ observations of a dust plume transported to the Mediterranean showed an electrically charged dust plume coinciding with long-range coarse particle transport and it is speculated that the charging influenced the coarse particle transport (Renard et al., 2018). This process is not considered or represented in GCMs.

Convective mixing within the Saharan air layer (SAL): Repeated convective cycling over several days could mix dust particles throughout the depth of the SAL after they have settled lower during the nighttime (Gasteiger et al., 2017; Xu et al., 2018); during the daytime, solar heating drives convective mixing, distributing dust of all sizes throughout the SAL.

This has been hypothesised and tested in modelling of the SAL, where it was found that vertical mixing within the SAL was a common phenomenon which could enhance vertical mixing of coarse dust, and thus, horizontal transport distance (Gasteiger et al., 2017). Lu et al. (2023) observed a diurnal cycle in the aerosol optical centroid height in the SAL using satellite observations, with higher values around midday, which suggests that the diurnal cycle in solar heating has an important effect on the vertical structure of dust in the SAL, supporting the influence of convective mixing on coarse dust transport and vertical distribution. The importance of convective mixing on coarse particle transport has also been shown in modelling of the Tibetan Plateau (Xu et al., 2018). In this context, the strength of daytime convective mixing as a result of solar heating could influence the extent to which dust is recirculated vertically within the SAL; the stronger the updraft, the greater the size of particles that can lofted, and thus transported greater distances.

Turbulent mixing: Turbulence could mix particles up through, and above, the boundary layer (BL), transporting dust away from the surface. Field campaigns have observed updrafts an order of magnitude greater than the settling velocity of 8 µm particles (Denjean et al., 2016). Large-eddy simulations (LES) with resolved turbulence (as opposed to parameterised turbulence in GCMs) have shown improved simulated coarse dust transport representation relative to lower resolution models (Cornwell et al., 2021; Rodakoviski et al., 2023).

Self-lofting: The SW absorption of dust heats the air around it, creating positive buoyancy, potentially resulting in the ascent of dust layers higher in the atmosphere (Boers et al., 2010; Colarco et al., 2014). Dust plumes could be more susceptible to this process than previously thought due to (a) increased presence of coarse particles which are more absorbing than smaller dust particles (Adebiyi and Kok, 2020), (b) particle mineralogy resulting in more absorbing dust than previously thought, or size-resolved mineralogy resulting in increased absorption from larger particles (Di Biagio et al., 2020; Li et al., 2021), and (c) aspherical particles altering the optical properties. The process of self-lofting has been demonstrated for other types of absorbing aerosols such as volcanic ash and biomass burning (Boers et al., 2010; Johnson and Haywood, 2023; Khaykin et al., 2022). While self-lofting is represented in GCMs via aerosol-radiation interactions, representations of dust self-lofting are dominantly limited by uncertainty in dust absorption, which is influenced by shape, size and mineralogy.

Topography-enhanced vertical transport: Gentle topography near source can enhance the initial vertical transport of dust, raising it more quickly towards regions of the atmosphere with larger-scale convective motions. This has been postulated to be the cause of enhanced dust concentrations during a field campaign (Rosenberg et al., 2014), and in satellite observations and reanalysis data (Xu et al., 2018). GCMs, with their grid resolution of O(100 km), may be missing this process by not representing subgrid-scale topography effectively or at all, whereas LES experiments with gentle topography (50–100 m tall × 1 km long) show improved vertical transport of coarse dust particles (Heisel et al., 2021).

A lack of understanding of these processes means we are still not able to fully explain the physical processes behind long-range coarse dust transport. In models, gravitational settling of dust is typically governed by the Stokes velocity, which controls the downwards transport of aerosol mass between model layers throughout the atmosphere as a result of

gravity (Seinfeld and Pandis, 2016). This is distinct from the process of deposition, which defines the mass of aerosol removed from the atmosphere and deposited to the Earth's surface. Recent research has examined the impact of reducing the sedimentation velocity (i.e., Stokes) or density of dust in models in order to bring the model into agreement with the observations. Drakaki et al. (2022) found that sedimentation of coarse particles had to be reduced by 40 %–80 % in order to be bring an NWP model into agreement with observations at the Sahara and east Atlantic. Meng et al. (2022) reduced particle density from 2500 kg m^{-3} to as low as 125 kg m^{-3} to improve model coarse size distributions, effectively reducing the sedimentation rate by 95 %. However, no studies have performed a comprehensive examination of all dust transport processes represented in a climate model in terms of retention of coarse dust in the atmosphere.

In this study, we test the sensitivity of different processes governing the transport and deposition of coarse dust particles (sedimentation, impaction scavenging, turbulent and convective mixing, and altered dust SW absorption) in a climate model with a resolution of 1.875° × 1.25° (∼ 190 km at 20° N). We aim to better understand which processes have the most influence on the transport and deposition of coarse dust within the model with a view to constraining changes which could be implemented to improve coarse dust transport. In Sect. 2, the methodology of these model experiments is explained. Section 3 presents results of each sensitivity experiment, which are discussed in-depth in Sect. 4. Finally, in Sect. 5, we conclude that sedimentation is the overarching process by which coarse dust transport is governed in the model.

2 Methodology

2.1 Model configuration

An atmosphere-only version of the Hadley Centre Global Environment Model 3 (HadGEM3-GA7.1; Walters et al., 2019) is used in this study. The model uses fixed observed sea surface temperatures (SSTs) but is otherwise free-running. The model configuration has a nominal horizontal resolution of 1.875° × 1.25° (∼ 190 km at 20° N), 85 height levels, of which 29 are below 6 km altitude, and 20 minute time steps. Land surface fields are calculated by the Joint UK Land Environment Simulator land surface model (JULES; Walters et al., 2019). In this study, we analyse monthly averaged simulation data for June of each year, spanning a total of 20 years (1995–2014) for each experiment. June was selected as it is one of the dustiest months in the Sahara and coincides with two of the three aircraft campaigns (Fennec and SALTRACE; see Sect. 2.3) used in this study for comparison with the model.

Table 1. Diameter (d) range, representative diameter (D_{rep}) also known as the geometric mean diameter, and wet scavenging coefficient (Λ) of the modelled mineral dust size bins in the CLASSIC dust scheme described in Woodward (2001).

Size bin	Diameter range (µm)	Representative diameter (µm)	Scavenging coefficient
1	$0.0632 \le d < 0.2$	0.112	2×10^{-5}
2	$0.2 \le d < 0.632$	0.356	2×10^{-5}
3	$0.632 \le d < 2$	1.12	3×10^{-5}
4	$2 \le d < 6.32$	3.56	6×10^{-5}
5	$6.32 \le d < 20$	11.2	4×10^{-4}
6	$20 \le d < 63.2$	35.6	4×10^{-4}

2.1.1 Dust emission scheme

Mineral dust is represented using the Coupled Large-scale Aerosol Simulator for Studies in Climate (CLASSIC) scheme (Woodward, 2001; Woodward et al., 2022). Dust in the model is called at every time step using driving fields from the atmospheric and land surface components of the model (Woodward et al., 2022). The horizontal (G) and vertical (F) dust mass fluxes (both in kg m^{-1} s^{-1}) are derived using the method of Marticorena and Bergametti (1995). G is calculated in each of the nine logarithmically-spaced size bins (i) between 0.0632 and 2000 µm diameter, using the following,

$$G_{(i)} = 2.61 \rho B U^{*3} \left(1 + \frac{U^*_{t(i)}}{U^*}\right)\left(1 - \left(\frac{U^*_{t(i)}}{U^*}\right)^2\right)\frac{M_{(i)}E}{g} \quad (1)$$

where ρ is the air density (in kg m^{-3}), B is the grid cells' bare soil fraction, U^* is the surface layer friction velocity (in m s^{-1}), U^*_t is the threshold friction velocity (in m s^{-1}) from Bagnold (1941) with corrections for the effect of soil moisture based on Fecan et al. (1999), M_i is the ratio of dust mass in the size division i to the total mass based on HWSD data (Nachtergaele et al., 2008), g is the acceleration due to gravity (in m s^{-2}), and E is a dimensionless tunable parameter (see Sect. 2.1.5). Although the horizontal surface dust flux (G) is calculated for 9 size bins, the vertical dust emission flux (F) is only calculated for size bins 1–6 (up to 63.2 µm diameter; Table 1) which are emitted into the atmosphere to undergo further transport and mixing. G is solely used to determine the vertical dust mass flux (F) for dust emission, and is not connected to transport in the atmosphere. Wind-related parameters in Eq. (1) are extracted from model meteorology; bare soil fraction is extracted from model grid cell surface type.

The total vertical mass flux is related to the total horizontal flux across all nine size bins according to the method of Marticorena and Bergametti (1995). The vertical dust mass flux (F) for $i = 1, 6$ follows the size distribution of the hori-

zontal flux (Woodward et al., 2022), whereby the ratio of the sums ($\Sigma_{i=1,9}$ and $\Sigma_{i=1,6}$) redistributes the emitted mass into the six transported model bins.

$$F_{(i)} = 10^{(13.4F_c - 6.0)} G_{(i)} \frac{\Sigma_{i=1,9}(G_{(i)})}{\Sigma_{i=1,6}(G_{(i)})} \quad (2)$$

where F_c is the soil clay fraction based on Nachtergaele et al. (2008) which is constrained to a maximum of 0.1 based on Gillette (1979) and Alfaro and Gomes (2001), as described in Woodward et al. (2022).

2.1.2 Dust radiative interactions

In HadGEM3-GA7.1, the interaction of dust with radiation can be switched on or off. When switched on, the dust impacts atmospheric radiative fluxes and radiative heating rates, altering model meteorology, such as wind and temperature profiles, and subsequently modifying dust emissions, transport and atmospheric concentration. When switched off, dust does not impact meteorology, meaning the dust emissions and model meteorology can be kept the same across multiple simulations.

With dust radiative interactions switched on, dust can interact with radiation in both the SW and LW spectral regions. Each dust size bin is treated independently by the radiation scheme, with prescribed values for mass absorption efficiency, mass scattering efficiency (both in $m^2\,kg^{-1}$), and asymmetry parameter for each size bin in six and nine different spectral bands for the SW and LW, respectively. The values for the mass scattering efficiency, mass absorption efficiency, single scattering albedo (SSA), and phase function are shown in Table 3 in Sect. 2.2. These optical properties are calculated using refractive indices from Balkanski et al. (2007) and are given in the appendix of Bellouin et al. (2011). Dust is assumed to be spherical. Since the absorption and scattering depend on the amount of dust mass in each size bin (Table 3), the total scattering and absorption coefficient (in m^{-1}) of transported dust varies with the modelled dust size distribution and mass concentration, and hence varies throughout the dust transport process.

2.1.3 Atmospheric mixing of dust

Dust is mixed through the atmosphere by (dry and moist) convective mixing (CM) and turbulent mixing (TM). Figure 1 shows a simplified schematic of the model processes which impact dust during transport, including showing the approximate regions that both CM and TM act within the model atmosphere. The convection scheme in HadGEM3-GA7.1 represents sub-grid-scale transport of heat, moisture and momentum. The parameterised convection is responsible for both upwards and downwards movements of dust throughout the whole model atmosphere (Lock et al., 2000), and is based on the mass flux scheme of Gregory and Rowntree (1990). Downdrafts and convective momentum transport

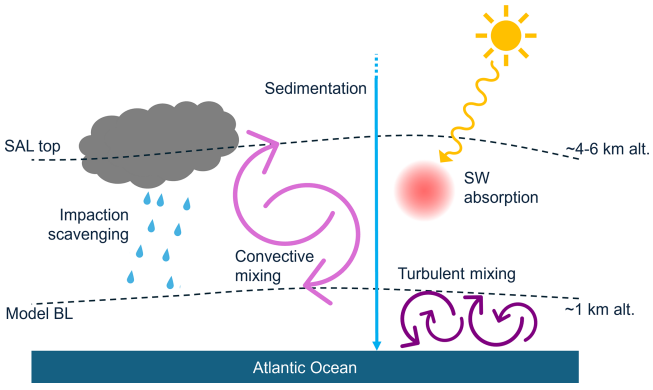

Figure 1. Schematic of the processes affecting dust transport and deposition in the model which have been altered in this study. The two horizontal dashed lines represent the model defined boundary layer (BL) top at ~ 1 km altitude and the SAL top at ~ 4–6 km.

are also included (Gregory and Allen, 1991). The interaction of CM with dust is not size-dependent in the model. TM is parameterised as a first-order closure (Lock et al., 2000), with additions from Brown et al. (2008) and Lock (2001). TM acts throughout the model BL, triggered at the surface by heating and wind shear, as well as at cloud-tops caused by radiative and evaporative cooling. Additionally, TM at the model BL top is via an entrainment parameterisation. The top of the model BL is typically ~ 1.2 km altitude at the Sahara and between 0.5–0.7 km altitude over the ocean. The model-defined BL is not the same as (e.g.) the SABL, which is much deeper layer extending up to ~ 6 km latitude as a result of surface-heating-induced dry convective mixing at the Sahara (Cuesta et al., 2009). In this case, the model BL height identifies where the character of mixing and application of sub-grid model physics processes change.

The effect of TM on dust is size-dependent in the model due to the inclusion of the effects of Brownian motion and inertial effects (equations in Sect. 2.1.4). In the analysed region in this study, TM is most active within and just above the model-defined BL, and CM impacts on dust are most noticeable above the model BL in the SABL and in the SAL as shown in Fig. 1. More details on the turbulence and convection schemes are in Walters et al. (2019).

2.1.4 Dust deposition processes

Above the model BL and the turbulent mixing maximum height, dust is subject to gravitational sedimentation at the Stokes velocity (V_S; in $m\,s^{-1}$). Within and just above the model BL, gravitational settling is combined with turbulent mixing, according to Eq. (3) (Woodward, 2001). Dust can experience dry deposition from the two lowest model levels in each time step through sedimentation and TM. Dry deposition velocity (V_D; in $m\,s^{-1}$) is represented using an inverse resistance analogue method (Seinfeld and Pandis, 2016)

$$V_D = (R_A + R_B + R_A R_B V_S)^{-1} + V_S \quad (3)$$

where R_A is the aerodynamic resistance (in s m^{-1}) and R_B is the resistance of the quasi-laminar surface layer (in s m^{-1}). R_A is a function of the wind speed, atmospheric stability and surface roughness, and is thus not dependent on particle size. R_B, also known as the surface layer resistance, is the resistance experienced by the particles in the laminar sublayer adjacent to the surface and is therefore based on molecular scale transport incorporating particle motion by both Brownian diffusion and inertial effects. R_B is calculated

$$R_B = \frac{1}{U^* \left(Sc^{-2/3} + 10^{-3/St}\right)} \quad (4)$$

where Sc is the Schmidt number and St is the Stokes number. The Stokes number (St) is a dimensionless characterisation of the behaviour of a particle in a fluid flow and represents the inertial effects, whereas the Stokes deposition velocity (V_S; used in calculating St) is the terminal velocity at which the particle settles within a fluid.

$$St = \frac{U^{*2} V_S}{g \upsilon_{air}} \quad (5)$$

where υ_{air} is the kinematic viscosity of air (in Pa s^{-1}). V_S is calculated based on the method by Pruppacher and Klett (2010)

$$V_{S(i)} = \frac{{D_{rep(i)}}^2 g \rho_p C_c}{18 \mu_{air}} \quad (6)$$

where D_{rep} is the representative diameter (size bin values in Table 1; in µm), ρ_p is the particle density (in g m^{-3}), C_c is the Cunningham correction factor, and μ_{air} is the dynamic viscosity of air (in Pa s^{-1}). C_c has a dependency on D_{rep} and accounts for slip flow and can impact the deposition rate of fine particles below 1 µm diameter by up to 10 %.

Wet deposition of dust can occur through impaction scavenging (IS) by precipitation below-clouds (in kg m^{-2} s^{-1}). In the model, wet deposition is composed of two diagnostics, wet deposition by convective precipitation and by large-scale precipitation, which are collated and treated as one in this study. The rate of IS is controlled by a dimensionless scavenging coefficient (Λ), the precipitation rate (P), and dust mass concentration (C) using the equation

$$\frac{\delta C_{(i)}}{\delta t} = -\Lambda_{(i)} P C_{(i)} \quad (7)$$

The values of Λ for each size bin, i, are shown in Table 1 and generally increase with the particle diameters represented in HadGEM3-GA7.1. These values are based on experimental measurements by Volken and Schumann (1993) and have more recently been corroborated by Laakso et al. (2003). More information on the IS scheme is given in Jones et al. (2022).

2.1.5 Model Tuning

Ratcliffe et al. (2024) showed that the CMIP6 configuration of HadGEM3-GA7.1 significantly underestimates the mass loading of coarse dust from emission and this is exacerbated with long-range transport. Thus, to better understand the causes of this growing underestimation, we have tuned the model's dust emissions to start with a better estimation of the real-world dust size distribution based on observations from the Fennec airborne field campaign. The Fennec campaign measured vertically-resolved dust particles up to 300 µm diameter in the atmosphere over the northwestern Sahara during June 2011 (Ryder et al., 2013b). Only particles observed within the model size range are used for comparison here (0.0632–63.2 µm). The tuning of the model is to account for processes not included in the model, such as wind gustiness at the source, and the relationship of soil moisture in the model's top soil level and at the soil surface, as well as for the effect of spatial and temporal averaging onto grid box areas and model time steps (Woodward et al., 2022). There are three tuning parameters which can be varied to achieve this: a global multiplier of horizontal dust flux (E, used in Eq. 1; changed from 2.25 to 30), a friction velocity multiplier (k_1; reduced from 1.45 to 1.1), and a top level soil moisture multiplier (k_2; unchanged at 0.5). The tuning factors have no size dependency. k_1 is used in the calculation of U^*, directly altering the model friction velocity (U^*_M; in m s^{-1}) (Woodward et al., 2022).

$$U^* = k_1 U^*_M \quad (8)$$

k_1 is used to account for spatial and temporal averaging resulting from the fact that the driving fields for the dust scheme are the model's grid box mean time step mean values, whereas the values used in Eq. (1) are based on shorter timescale measurements at single locations. Reductions in k_1 result in reductions in the emitted fine fraction of dust; this is a consequence of the size dependence of U^*_t which is a roughly U-shaped curve with a minimum at $\sim$ 50 µm diameter (Bagnold, 1941). Thus, lower U^* predominantly impacts the finer particles which have a higher threshold friction velocity to overcome. k_2 is used in the calculation of the volumetric soil moisture (ω) as in Woodward et al. (2022).

$$\omega = k_2 \omega_1 \quad (9)$$

where ω_1 is the grid box mean soil moisture in the top soil level (in kg m−2). ω feeds into the relationship between the threshold friction velocity for moist soil (U^*_t) and the dry threshold friction velocity (U^*_{td}) by

$$U^*_t / U^*_{td} = 1 \quad \text{for } \omega < \omega'$$
$$U^*_t / U^*_{td} = \left(1 + 1.21(\omega - \omega')^{0.68}\right)^{0.5} \quad \text{for } \omega > \omega' \quad (10)$$

where $\omega' = 0.14 F_c^2 + 17 F_c$. Tuning with k_2 is used to account for the difference between the soil moisture in the

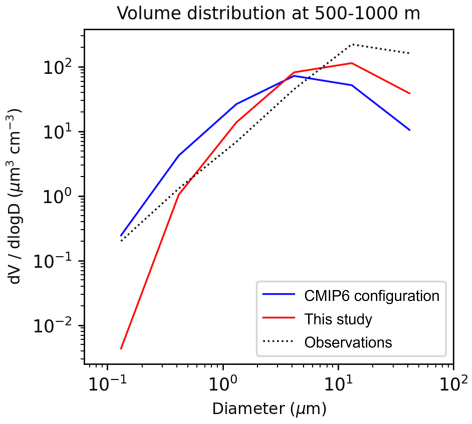

Figure 2. VSD between 500–1000 m altitude at the western Sahara for the configuration used in this paper (red), the model tuning used in the HadGEM3-GA7.1 CMIP6 configuration and in Ratcliffe et al. (2024) (blue), and the Fennec airborne in-situ mean dust size distribution in the same model size bins (between 0.0632–63.2 µm) over Mauritania and Northern Mali (Ryder et al., 2013b) (black dotted).

model's 10 cm deep top soil level and that at the surface, again accounting for spatial and temporal averaging. The tuning factors only impact the emission of dust (not subsequent transport). We have tuned the model to emit a coarser dust size distribution, which brings the coarse and super-coarse volume size distribution (VSD) into better agreement with the Fennec observations (Fig. 2). The tuning is based on observations of near-surface dust concentrations (e.g., Prospero et al., 2010), AOD (from AERONET (AErosol RObotic NETwork; Holben et al., 2001) and MODIS (Moderate Resolution Imaging Spectroradiometer; Levy et al., 2013)), and Fennec airborne in-situ mean dust size distributions over Mauritania and Northern Mali (Ryder et al., 2013b). The improved coarse VSD at the source will mean our investigation into the loss of coarse material over transport is less affected by a reduced coarse fraction bias at emission. For this study, we assume that the Fennec data is representative of Saharan dust emissions. The tuning carried out for this study is based purely on the Sahara and trans-Atlantic dust transport, considering no other sources across the globe and is thus only suitable for the purposes of this study.

2.2 Model experiments

In order to test the sensitivity of coarse dust transport in the model, we have removed or scaled the impact of various relevant dust transport processes. Figure 1 shows the relevant processes in the model atmosphere impacting mineral dust transport and deposition. Two control experiments are used, firstly one with dust radiative effects (RE) turned off, (Control), where experiments have identical meteorology and dust emissions, and secondly one with dust RE turned on (i.e. emissions and atmospheric circulation vary between simulations; see Sect. 2.1.2, REControl). Including the Control, nine simulations have been performed in an RE off setup with changes to transport and deposition mechanisms (experiments listed in Table 2). Two simulations were run with RE on, REControl and one in which the SW absorption of dust has been tripled.

Table 2. Sensitivity experiments, abbreviations, and dust radiative interactions on/off.

Simulation name	Abbreviation	RE on/off
Radiative effects Off Control	Control	Off
No sedimentation	NoS	
95 % reduction in sedimentation	0.05S	
80 % reduction in sedimentation	0.2S	
50 % reduction in sedimentation	0.5S	
No impaction scavenging	NoIS	
No convective mixing	NoCM	
Doubled convective mixing	2×CM	
No turbulent mixing (over the ocean)	NoTM	
Radiative effects On Control	REControl	On
Tripled SW absorption	3×SW	

When interacting with radiation, dust is able to influence radiative heating, and therefore regional meteorology, which subsequently impacts dust emissions, atmospheric dust concentration and transport. Therefore, most of the experiments are run with RE off in order to ensure identical emissions and meteorology and so that the impact of the sensitivity test is the only changing feature and can be directly assessed. The exception is the SW absorption sensitivity test, which requires radiative interactions to be switched on in order to allow the changes in dust absorption to affect radiation fields. This introduces the potential for different evolutions of atmospheric dust to impact circulation differently between REControl and 3×SW. This is discussed further in Sect. 2.1.2.

Firstly, we aim to test reductions in the sedimentation velocity (also simply sedimentation) of dust in the HadGEM3-GA7.1 climate model configuration. Alterations to the sedimentation in this study are hypothesised to act as a proxy to processes or mechanisms in the real-world which reduce the settling velocity of the particles, such as asphericity and electrical charging. Sedimentation affects dust in all levels of the model throughout the atmosphere. To vary the sedimentation, the Stokes velocity, V_S (appearing in Eq. 3 for calculating the dry deposition velocity), is altered in the UM and JULES code. Unlike other experiments in this study, changes were implemented in the surface model (JULES) code as V_S is used in the calculation of the Stokes number (St; Eq. 5), which is used to calculate surface layer resistance (R_B; Eq. 4) in JULES. Four simulations with reductions to the sedimentation of dust are run. One experiment tested the effect of removing sedimentation completely (NoS), in this case, V_S is overwritten to equal 0 at all times and locations in the model. In other experiments, the Stokes velocity V_S is

reduced by 50 % (0.5S), 80 % (0.2S), and 95 % (0.05S) (Table 2); in these cases, V_S is simply multiplied by 0.5, 0.2, and 0.05, respectively. These changes are on the order of magnitude of changes made by Drakaki et al. (2022) and Meng et al. (2022) in their experiments testing reduced sedimentation and particle density.

We test the impact of removing CM on dust (NoCM) as well as the impact of doubling the effect of CM (2×CM). We also test the impact of removing TM of dust from the model (NoTM). As TM contributes to the uplift and emission of dust over land in HadGEM3-GA7.1, we employ a grid box land cover mask to keep TM turned on over land, but turned off over the ocean. TM appears in the calculation of the dust deposition velocity in the BL (Eq. 3) in the form of R_A and R_B, the aerodynamic and quasi-laminar sublayer resistances, and thus we reduce R_A and R_B to 0 to represent a NoTM environment. It is important to note that in neither of these experiments (NoCM and NoTM) are we removing these mixing mechanisms from the model, only their interactions with dust transport and deposition.

One simulation is performed to test the sensitivity of coarse dust to wet deposition in the model. Values of the prescribed scavenging coefficient, Λ (in Eq. 7 and Table 1), are set to 0 for all size bins in a "no impaction scavenging" experiment (NoIS).

In the final sensitivity experiment, we have tripled the SW absorption of dust (3×SW) as a large change to understand if there is any sensitivity to size resolved transport through SW heating-induced self-lofting in the model. The nature of this change relating to the RE means this experiment is carried out in a simulation with RE turned on. The original values for the SW mass absorption efficiency of dust have been tripled at all wavelengths (original and tripled values at 550 nm wavelength shown in Table 3). Scattering mass efficiency remains unchanged. The LW RE and optical properties remain unchanged. Due to the unchanged scattering properties, the single scattering albedo (SSA; the ratio of scattering to extinction) is lower in the 3×SW experiment compared to REControl, especially at coarser size ranges, demonstrating the increased absorption.

Model data is averaged over box regions related to the location of in-situ airborne campaign data used in this study for evaluation. Additionally, we use a trans-Atlantic transect slicing through the centre of the mean summer dust plume to analyse changes along a consistent latitude. These regions are shown in Fig. 3. The box regions correspond to those used in Ratcliffe et al. (2024).

2.3 Observations

To evaluate the model's vertically-resolved trans-Atlantic transport of mineral dust, we use in-situ observations of the full dust size distribution from three airborne field campaigns between the western Sahara and Caribbean. The Fennec campaign provides measurements over the western Sahara and Canary Islands, taken during June 2011 (Ryder et al., 2013b, a). The AERosol properties – Dust (AER-D) campaign measured dust near Cape Verde during August 2015 (Ryder et al., 2018). Finally, the Saharan Aerosol Long-range Transport and Aerosol-Cloud-Interaction Experiment (SALTRACE) campaign measured dust at Cape Verde and the Caribbean in June–July 2013 (Weinzierl et al., 2017). Together the campaigns provide the full dust size distribution over 111 vertical profiles up to 8 km altitude. Only measurements within the bounds of the model size bins are analysed for this study ($0.0632 < d < 63.2\,\mu m$). These profiles are used in this study to assess the vertical distribution of dust in the model simulations. All observed concentrations are at ambient conditions. Descriptions of the processing carried out on the data are the same as in Ratcliffe et al. (2024) where additional details can be found.

Comparisons between observations and models are complex for many reasons, including differences in both temporal and spatial scales. Previously, Ratcliffe et al. (2024) assessed how representative of "normal conditions" these campaigns are and whether any bias in data collection is large enough to skew comparisons, and found that these campaigns are suitable for climatological comparisons. We use 20 monthly June averages (1995–2014) from the model in order to create a model average representative of a climatology.

3 Results

3.1 Comparison of modelled size distributions against aircraft observations

Here we compare the VSD and vertical profile of dust mass against aircraft observations from field campaigns at four locations representing the transport lifecycle of dust. Figure 4 shows the mean VSD between 2–4 km altitude in each of the experiments and from the three field campaigns at four locations. Figure 5 shows the normalised total mass profiles of the observational data and all RE off experiments, and the dust mass median altitude (MMA) of the model experiments over the depth of the model atmosphere: the altitude at which 50 % of the mass is below and 50 % is above (Lu et al., 2023).

First, we compare the Control with the observations: the Fig. 4 VSD shows that the model significantly underestimates coarse dust mass, particularly in the largest two size bins, 6.32–20 and 20–63.2 µm. The extent of the underestimation becomes worse during long-range transport and is especially depleted (1 order of magnitude and 7 orders of magnitude less than observations for the two largest size bins respectively) at the Caribbean (Fig. 4d). This shows that regardless of emissions tuning in the model to improve agreement at the Sahara, a significant under-representation of super-coarse and giant dust exists in the model throughout trans-Atlantic dust transport, driven by rapid deposition of coarse particles, as explored in more detail by Ratcliffe et al. (2024). In terms of the vertical distribution of dust,

Table 3. Mass scattering efficiency (in $m^2\,kg^{-1}$), mass absorption efficiency range (in $m^2\,kg^{-1}$), single scattering albedo (SSA), and asymmetry parameter at 550 nm wavelength including the original values and those used in the 3×SW experiment.

Size bin	Mass scattering efficiency ($m^2\,kg^{-1}$)	Mass absorption efficiency ($m^2\,kg^{-1}$)		SSA		Asymmetry parameter
	Original	Original	3×SW	Original	3×SW	Original
1	998.61	16.94	50.83	0.98	0.95	0.35
2	3657.38	28.19	84.56	0.99	0.98	0.71
3	897.40	29.99	89.97	0.97	0.91	0.69
4	237.31	21.70	65.09	0.92	0.78	0.80
5	62.15	15.32	45.96	0.80	0.57	0.86
6	15.23	8.65	25.96	0.64	0.37	0.92

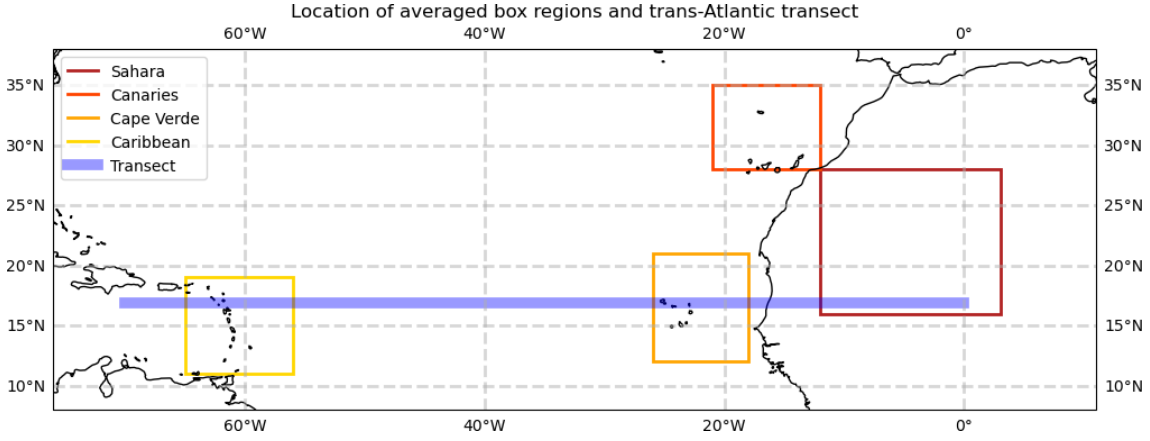

Figure 3. Map showing the location of box regions used for averaging model data in this study, as well as a transect covering the trans-Atlantic dust plume.

Fig. 5 shows that the general structure of the model profile agrees with the observations. At the Sahara, there is little difference in VSD shape and magnitude between the Control, 2×CM, NoCM and NoTM experiments at any size range (Fig. 4a). Compared to the Fennec observations, these experiments underestimate the fine particle VSD below 0.632 µm and the coarse particles' VSD above 6.32 µm. The model underestimates the mass of dust below 3.5 km compared to the observations, and overestimates the mass above this altitude (Fig. 5a). This could be due to the underestimation of coarse volume shown in Fig. 4a. At the Canaries and Cape Verde, there is a tendency to model the dust too low in the atmosphere.

The NoIS experiment is the only experiment to have a dominant and large impact on the fine particles, with an increase in fine VSD of more than one order of magnitude at the Sahara (Fig. 4a). At diameters larger than 20 µm, there is minimal impact from the removal of impaction scavenging. Changes in VSD within the fine size range represent much greater changes in number distribution due to the smaller size and thus, volume. The increase of one order of magnitude of VSD represents a much greater change to the number concentration of fine particles in the NoIS experiment; the 0.0632–0.2 µm (size bin 1) number concentration in the SABL is 2000 % greater compared to the Control (not shown). At the Caribbean, the removal of IS brings the magnitude of the VSD of size bins 1–4 into better agreement with the SALTRACE-W observations than any other experiment. The NoIS experiment also significantly changed the shape of the vertical profile of total dust mass (Fig. 5). With long range transport, the difference of the NoIS profile to the other experiments becomes clearer, with decreased relative dust mass concentration within the SAL, and increased mass above the SAL (> 5 km altitude at Cape Verde and > 4 km at the Caribbean). At the Caribbean (Fig. 5d), the MMA of the NoIS experiment (2546 m altitude) is 500 m higher than the next experiment (NoS), and 700 m higher than the Control.

The sedimentation experiments have the greatest impact on the VSD at coarser size ranges, predominantly impacting size bins 5 and 6 (6.32–63.2 µm; Fig. 4). The larger the change to sedimentation, the greater the increase in coarse particle VSD. At the Sahara, the NoS VSD is nearly 2 orders of magnitude greater in the 20–63.2 µm size bin than the Control simulation. In terms of the VSD shape at the Sa-

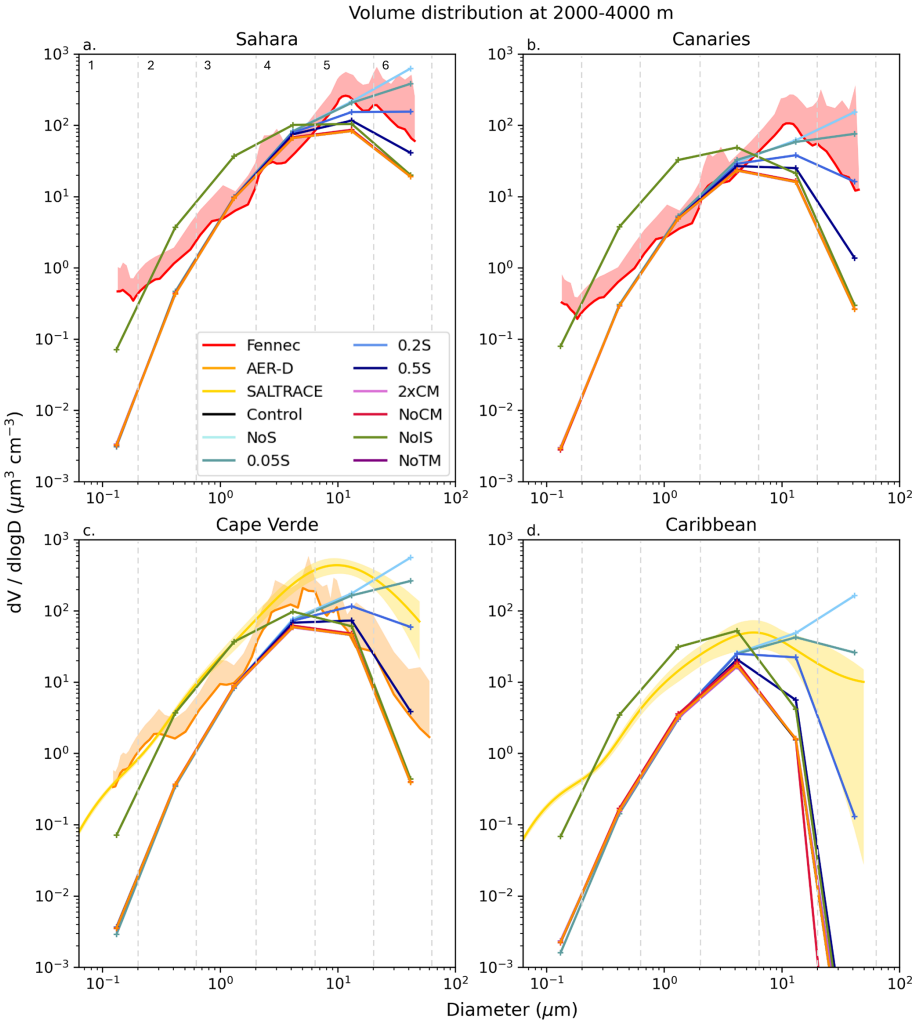

Figure 4. VSD (in $\mu m^3\ cm^{-3}$) from each model experiment and field campaign averaged between 2–4 km altitude shown at the Sahara **(a)**, Canaries **(b)**, Cape Verde **(c)** and Caribbean **(d)**. Grey dashed lines show the bounds of the model size bins, and their associated bin number (Table 1) are shown across the top of panel **(a)**. The shading above the Fennec and AER-D campaign VSDs represents one standard deviation. For clarity, the standard deviation shading is only shown above the line due to the logarithmic scale. Shading above and below the SALTRACE VSDs represents the 10th and 90th percentiles of the measurements. The Control simulation terminated at $3.57 \times 10^{-6}\ \mu m^3\ cm^{-3}$ in size bin 6 (20–63.2 µm) at the Caribbean. Where the Control simulation profile is less visible, it generally closely follows the NoTM experiment in all panels. The locations of the field campaigns and model box regions are shown in Fig. 3.

hara, the 0.5S and 0.2S experiments produce VSDs with a shape most similar to the observations, suggesting a 50 %–80 % reduction in sedimentation is required in order to bring the model into better agreement with the observations. Figure 5b, c, d show that decreasing the strength of sedimentation results in dust being transported at higher altitudes, with a decreased relative mass in the MBL.

In terms of sensitivity to sedimentation strength, at the Sahara all four of the sedimentation experiments and the Control have a VSD for 20–63.2 µm particles within 2 orders of magnitude of each other, however, upon transport to the Caribbean, they vary by 8 orders of magnitude. Without sedimentation, the NoS experiment raises the super-coarse VSD value by too much at all locations leading to an unrealistic VSD shape. Contrastingly, the effect of reducing gravitational settling by 50 % is not large enough to cause a noticeable difference to the super-coarse VSD from the Control at the Caribbean. The reduction in sedimentation required to bring the the coarse VSD into agreement with the observations increases with distance from the Sahara; a reduction of 50 %–80 % at the Sahara, Canaries and Cape Verde, and 80 %–95 % at the Caribbean is required.

As the VSDs of the NoTM, NoCM and 2×CM experiments closely follow the Control experiment, the disparity between these experiments and the observations grow at a similar rate to the Control with distance from the Sahara

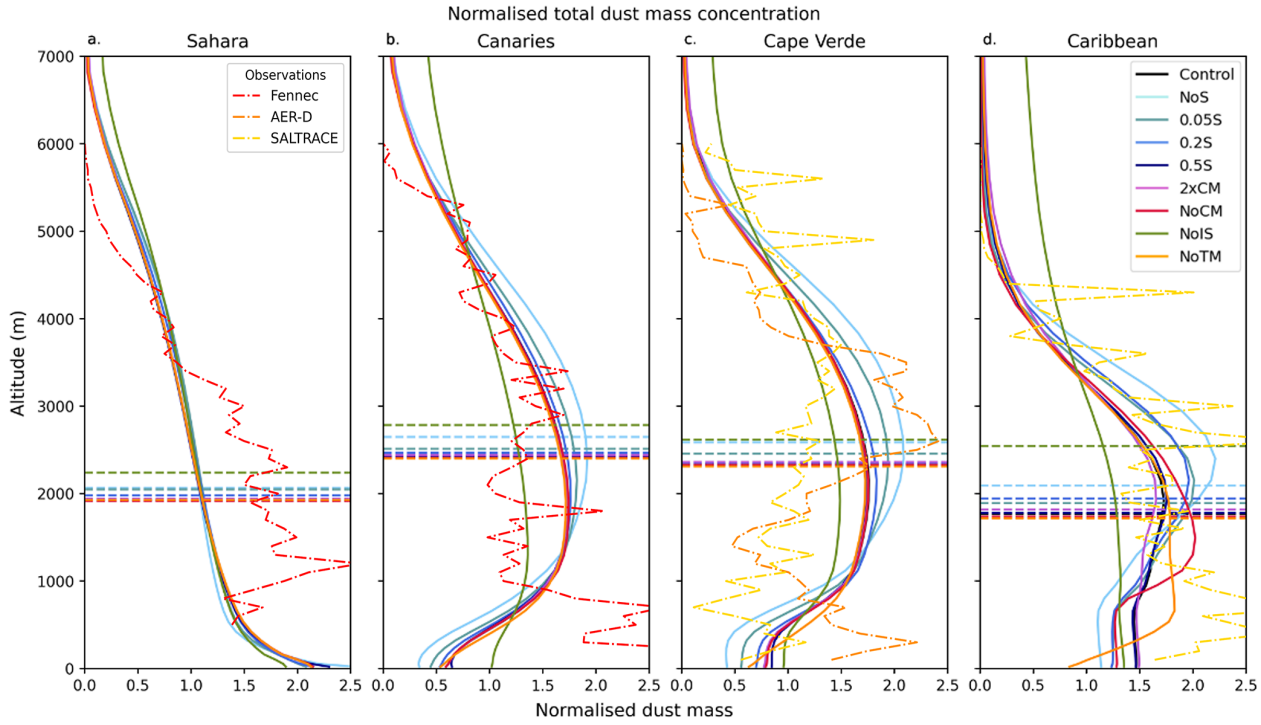

Figure 5. Normalised profile of total dust mass concentration (0.0632–63.2 µm diameter) from RE off model simulations (solid lines) and their respective total dust MMA (dashed horizontal lines). Observations from the in-situ aircraft campaigns, Fennec at the Sahara and Canaries (red), AER-D at Cape Verde (orange), and SALTRACE at Cape Verde and Caribbean (yellow), are shown up to 6 km altitude (dash dot lines). The model and observations profiles are normalised by the mean concentration over the depth of the model atmosphere and between 1–6 km respectively. Excluding the data below 1 km in the observations normalisation removes any influence by non-dust aerosols in the MBL. The MMA from the observations is not included due to the presence of non-dust aerosols in the MBL (below 1 km altitude) altering the value. Where the Control simulation profile is less visible, it generally closely follows the CM and 0.5S experiments in panels **(a)**, **(b)**, and **(c)**, and the 0.5S experiment profile in panel **(d)**.

(Fig. 4), except for at the Caribbean, where the NoCM VSD is 2 orders of magnitude lower than the Control experiment in the 20–63.2 µm size bin. While some experiments are similar in VSD to the Control, Fig. 5 shows that they have important changes in the vertical distribution of dust (e.g., NoTM and NoCM at the Caribbean) which are discussed further in Sect. 3.3 and 3.4.

Overall, VSD for the largest model size bins (20–63.2 µm) could only be brought into agreement with observations through large change to the sedimentation, which also resulted in trans-Atlantic transport at a greater altitude. Changes to CM and TM did not have strong enough effects on the coarse particle VSD in comparison. Finally, the NoIS experiment showed a dominant impact on the fine size bins, which significantly altered the vertical distribution of the dust, lofting it too high compared to the observations. The next section examines individual processes and experiments in more detail.

3.2 Sensitivity to Sedimentation Rate

As shown in Fig. 4, reductions to sedimentation result in the greatest impact on coarse dust size distribution. With reductions in sedimentation, coarse dust is retained in the model atmosphere for longer, as is shown by the increased VSD at the Caribbean. Figure 6 shows normalised size bin 6 mass concentration profiles in the Control and sedimentation experiments with their respective MMA's, and the normalised size bin 6 profiles from the in-situ aircraft campaigns.

By first looking at the MMA values, we can see that by decreasing sedimentation, the size bin 6 (20–63.2 µm) dust mass is transported higher within the model atmosphere. At the Sahara, the NoS MMA is more than 0.8 km higher than the Control MMA. At the Canaries and Cape Verde, the NoS MMA is between 1–1.5 km higher. At the Caribbean, a negligible mass of size bin 6 mass remains in the Control and 0.5S experiments, while the NoS experiment MMA is >2 km transporting significantly more super-coarse dust at higher altitudes.

At the Sahara, the general shape of the size bin 6 profile is not largely different between the five simulations (Fig. 6a),

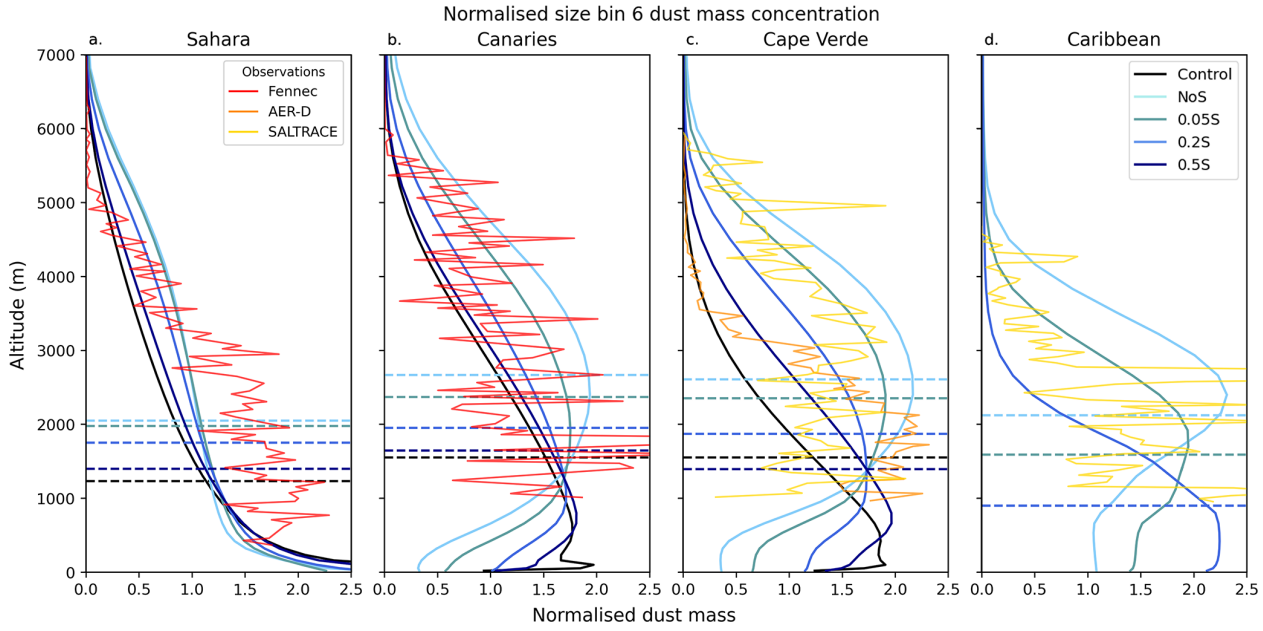

Figure 6. Normalised 20–63.2 µm (size bin 6) mass concentration profiles from the sedimentation and Control experiments, and the in-situ aircraft campaigns. Dashed horizontal lines show the size bin 6 MMA over the whole profile. The MMA from the observations is not included due to the presence of non-dust aerosols in the MBL (below 1 km altitude) altering the value. The profiles have been normalised relative to the mean size bin 6 mass concentration across the depth of the profile. Model mass concentrations less than 0.001 µg m^{-3} are not shown, and consequently the Control and 0.5S experiments are not included on panel **(d)**. Measurements from the MBL have been excluded from the observational profiles due to potential contamination of the results by non-dust species.

though the simulations with a greater reduction in sedimentation have relatively more mass between 1–6 km than the experiments with no or smaller reductions in sedimentation. Reductions in sedimentation also result in a slightly increased normalized mass above 1 km and decreased normalized mass beneath 1 km, indicating that more super-coarse dust reaches higher altitudes over the Sahara under reduced sedimentation. The observed size bin 6 profile from the Fennec campaign shows that the majority of mass is below 5 km altitude, with a greater relative mass below 3 km compared to the model experiments. At the Canaries and Cape Verde, there is a more noticeable difference in the profile shapes between the experiments (Fig. 6bc). In the Control, the mass is more concentrated closer to the surface, with no discernible evidence of the marine boundary layer (MBL) and SAL structure in the dust profile. However, as sedimentation decreases, the MMA rises, creating a profile with decreased dust concentration between 0–1 km associated with the MBL, and a peak in concentration in the SAL between 2–4 km altitude. At the Canaries, the Fennec observational profile generally has a slightly steeper profile than the model simulations possibly due to a more well-mixed SAL up to the inversion with the free atmosphere (∼ 5.7 km altitude). A reduction in sedimentation of 95 % or more creates too much of a "bulge" in the SAL which is not represented in the Fennec profile. A reduction in sedimentation of up to 80 % could be plausible at the Canaries, though it is not clear which profile has the best agreement with the observations due to the exclusion of observations in the MBL (due to potential contamination by non-dust aerosol species). At Cape Verde, the SALTRACE-E profile is qualitatively the most in agreement with the 0.05S and NoS experiments, with a strong peak in concentration between 2–4 km altitude. The AER-D campaign has a lower peak in size bin 6 concentration between 1–2 km altitude with low relative concentrations above 4 km. The specific shape of the AER-D profile does not perfectly agree with any one simulation; above 3 km, best agreement is with the Control simulation, however, the peak in concentration between 1–2 km is much more well-represented by the 0.2S experiment. At the Caribbean, the different experiments diverge further; negligible size bin 6 dust mass remains in the Control and 0.5S experiment, while contrastingly the NoS and 0.05S retain SAL-like structure with MMAs at ∼ 2.1 and ∼ 1.6 km. The 0.05S experiment appears to have the best agreement with the SALTRACE-W profile, as the NoS experiment transports dust too high, and the 0.2S experiment, too low.

Ratcliffe et al. (2024) found that the model configuration used in this study has a reasonable representation of total dust mass vertical distribution, but transports coarse dust particles too low within the model atmosphere. Here, we show that the greater the reduction in sedimentation, the higher the MMA of the size bin 6 dust mass, showing that reduced sedimentation in the model can improve agreement of the vertical dis-

tribution of coarse dust mass over long-range transport with observations.

The sedimentation experiments show that increasing reductions of sedimentation with distance are required in order to bring the model into better agreement with the observations. These results show that a sedimentation velocity reduction of at least 50 %–80 % at the Sahara, Canaries and Cape Verde, and 80 %–95 % at the Caribbean is needed to enable the vertical structure and horizontal transport of coarse particles to better match that of observations.

3.3 Sensitivity to Convective Mixing

Figure 7 shows the absolute difference in size-resolved vertical dust mass concentration between the NoCM and Control experiments across the Atlantic transect – at 16.9° N from 70° W (at the Caribbean) to 0° E (at the Sahara) as in Fig. 3. In size bins 2–4, there is an increase in mass concentration within the SABL and SAL relative to the Control, especially between 1–2 km in the mid- and west-Atlantic. This increase within the SAL in the NoCM experiment is accompanied by a decrease in concentration in the MBL and free troposphere. Without CM the dust is mixed less evenly through the depth of the SABL and SAL, nor is it mixed away – either downwards from the SAL base towards the MBL or upwards from the SABL and SAL into the free atmosphere. This allows dust to build-up within the SABL and SAL, especially in the lower SABL and SAL, in the NoCM experiment, depleting the concentration of dust in the MBL and free atmosphere. As the SAL top lowers with westward transport, the increased concentration of dust transported within the SAL becomes more concentrated, resulting in an enhanced difference relative to the Control simulation.

The mass concentration distribution in size bin 1 has a more unique reaction to the removal of CM, with an increase in concentration in the MBL and a decrease between 1–2 km altitude between 30–70° W (Fig. 7a). This suggests that the size bin 1 particles interact in a different way with the CM processes to the other size bins, the reasons for which are not clear. We hypothesize that this could be a result of size bin 1 being particularly susceptible to impaction scavenging or Brownian diffusion once it has preferentially accumulated in the lower SAL.

In size bins 5 and 6 (6.32–20 and 20–63.2 µm) over land (∼ 17–0° W), there is an increase in mass concentration in NoCM up to 4–5 km altitude, with a decrease in dust transported above these altitudes. This suggests that similarly to size bins 2–4 in NoCM, the particles are not as efficiently mixed out of the SABL, increasing concentrations within the SABL. These results are somewhat counter-intuitive as we might expect that lack of CM would result in weaker transport of coarse dust mass upwards within the SABL, though the model results in Fig. 7 show increased size bin 5 and 6 dust mass over the SABL in the absence of CM. The largest increases in mass for size bins 5 and 6 are closest to the surface, although we do see mass increases all the way up to the top of the SABL to 4–5 km altitude. In size bin 6, the mass of particles transported across the Atlantic is so small (< 10 % increase) in both the Control and NoCM experiments that the absolute difference plot shows a negligible difference, matching the negligible change in VSD shown in Fig. 4. In size bin 5, the increased concentration of particles within the SABL results in increased dust transported westwards, with slight increases within the SAL. There is an increased mass concentration within the lower SAL as the dust accumulates above the SAL-MBL inversion.

Size bins 5 and 6 have greater sedimentation velocities than the smaller size bins (Eq. 6), and are therefore able to sustain downwards transport through gravitational settling despite the removal of convective mixing (which contributes to mixing from the SAL to the MBL). This explains the different structure of changes to size bin 5 and 6 compared to the smaller size bins shown in Fig. 7; despite removing CM, sedimentation still removes the larger model particles very rapidly from the SAL. Size bin 6 only shows noticeable changes to mass concentration over land where removal of CM results in more accumulation of dust mass closer to the surface. A relative, percentage change shows up to a 10 % increase in size bin 6 mass as far as 45° W, though these changes are only to very small mass concentrations of dust (less than 0.001 µg m^{-3}). Dust in size bin 5 is somewhat retained within the lower SAL, so experiences slightly more prolonged westwards transport than bin 6, though it eventually settles into the MBL.

Removing CM restricts the vertical transport of dust to within the SAL in all size bins, reducing mixing into the free atmosphere and the MBL. Horizontal transport to the north, south, and east of the transect is also reduced (not shown), suggesting decreased mixing of dust out of the dust plume in all directions, further increasing the concentration of dust within the SABL/SAL, and thus the mass of dust transported to the the West Atlantic in some size bins. Figure 5d shows the normalised total dust mass profile of the NoCM experiment and the greater mass transported between 1–2 km altitude in the lower SAL. In terms of spatial dependence on CM, in size bins 2–4, the greatest increase in concentration occurs at distance from the Sahara, suggesting that the removed CM has a cumulative impact, growing with distance.

Next we examine the experiment with doubled CM. We postulate that if the amount of mixing in the SABL and SAL is increased, then the coarsest particles may be lifted to higher altitudes, which could extend particle lifetime. Figure 8 shows similar cross sections to Fig. 7, except showing the difference between the 2×CM and Control simulations.

In general, the 2×CM experiment has the opposite effect on vertical dust distribution to the NoCM experiment; mass concentration is increased in the free troposphere and MBL, and concentration is lower within the SAL in size bins 2–4 (Fig. 8bcd). Generally at the Sahara (east of ∼ 17° W on Fig. 8), most size bins (2–6) show decreased concentrations

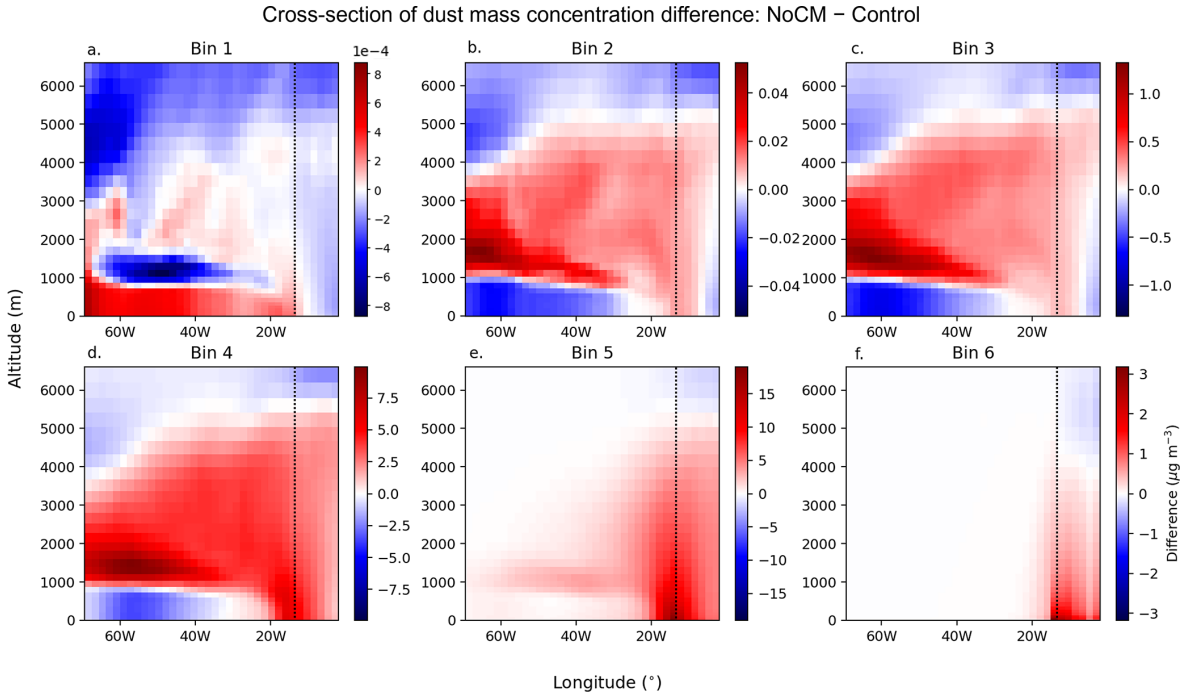

Figure 7. Impact of NoCM experiment: Cross section of difference between the size-resolved mass concentration in the NoCM and Control experiments in μg m^{-3}. At 16.9° N, the cross sections span from 70° W to 0° E, and extend up to 6.5 km. The colour bar scale varies between each plot. The vertical dotted line approximately locates the west African coast.

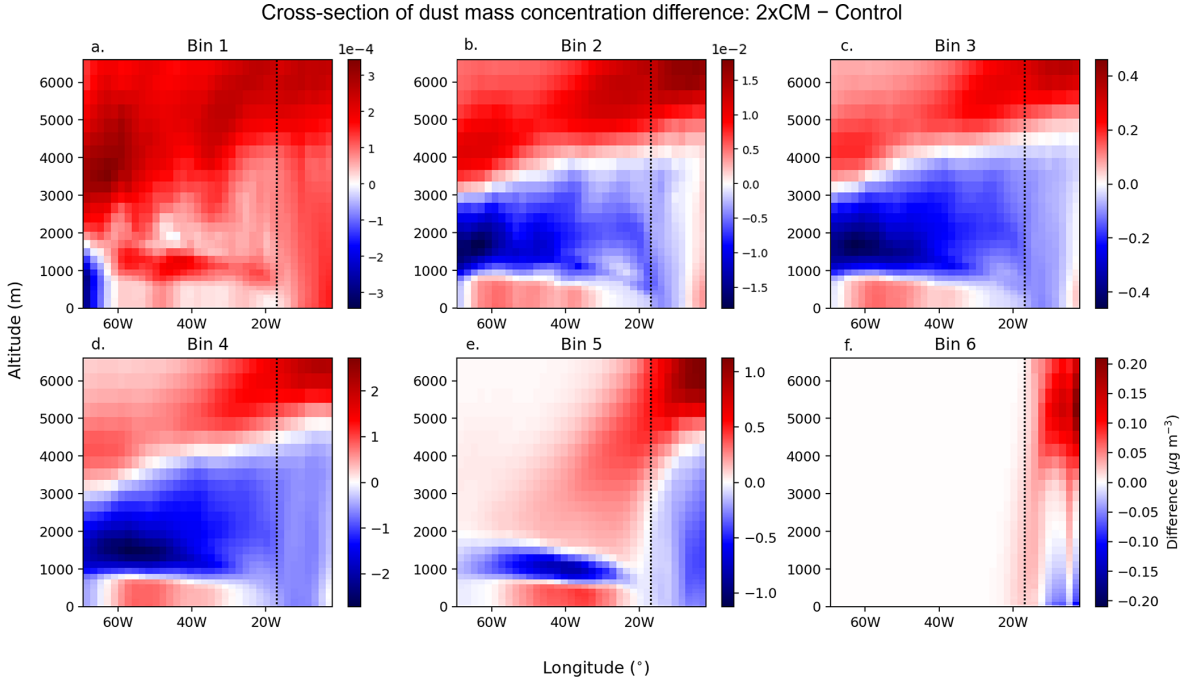

Figure 8. Impact of 2×CM experiment: Cross section of absolute difference between the size-resolved mass concentration in the 2×CM and Control experiments in μg m^{-3}. At 16.9° N, the cross sections span from 70° W to 0° E, and extend up to 6.5 km. The colour bar scale varies between each plot. The vertical dotted line approximately locates the west African coast.

below 4–5 km altitude, with increased dust mixed higher and out of the SABL to the free atmosphere. Size bins 5-6 show decreased dust mass concentrations in the SABL with increased concentrations above this, indicating that the doubled CM mixes dust efficiently in to the free atmosphere, out of the SABL. Within the SABL, dust concentrations are reduced the most close to the surface (size bin 6) and between around 500 m to 2 km (size bin 5) under doubled CM. This indicates that CM in the model is indeed affecting how high dust is mixed vertically within the SABL. However, with concentrations increasing above the SABL, this indicates that perhaps a doubling of CM is too large to match the required structure found in the observations.

All size bins show an increase in mass concentration above the SABL and SAL, and size bins 2–5 show an increase of dust mass in the MBL to 65° W (Fig. 8). This shows that with doubled CM, dust is more thoroughly mixed throughout and out of the SAL, reducing mass within the SABL and SAL, having an opposite effect to the NoCM experiment. The increase of size bin 5 dust in the upper SAL (above 2 km over the Atlantic) is caused by increased mixing to above the SABL over the Sahara followed by sedimentation down through the inversion at the SAL top and into the SAL, due to greater sedimentation in comparison to dust in size bins 2-4 which remain suspended predominantly above the SAL.

While the 2×CM experiment does result in additional upwards transport of dust, the extension of mixing is too great, mixing the dust beyond the SABL and SAL top, whereas in reality, dust transport is typically capped by a strong inversion at the top of the SABL and SAL with a sharp decrease in dust concentrations and noticeably less dusty atmosphere above (e.g. Ratcliffe et al., 2024; Ryder et al., 2019). In the NoCM experiment, the lack of CM resulted in dust transported too low within the SAL, also resulting in further divergence of the model vertical distribution to the observations. Although the CM changes investigated here are extreme, they provide an insight into the strength of these processes in governing coarse dust transport and have shown that CM is vital for determining the vertical distribution of dust in the model's atmosphere, especially the importance of CM for mixing dust across the temperature inversion separating the SAL and the MBL. This also has some effect on the horizontal distribution of the dust, but the main impact is on the vertical distribution of dust within the SAL, the MBL and the free atmosphere.

Conventional thinking is that once dust is emitted from the surface into the dry Saharan atmosphere, dry convection within the well-mixed SABL mixes dust from the surface up to high altitudes of around 5–6 km, above which dust concentrations are observed to drop sharply with the transition to the free atmosphere and a temperature inversion (Cuesta et al., 2009). In the SAL, dry convective mixing is again considered responsible for the well-mixed, elevated mixed layer characterising trans-Atlantic dust transport (Carlson, 2016). Thus we would expect increased CM to transport more dust upwards within the SABL, and retain more dust during transport within the SAL. However, instead we find that in the model, the large changes applied to CM here mean that CM's dominant role in dust transport is in mixing across the edges of dust layers and temperature inversions – across the SAL/MBL boundary, and the boundary between the top of the SAL and SABL into the free atmosphere. We also expect that in the model, CM acts both upwards and downwards, such that it may be possible that the net impacts of increased CM are negligible on upwards dust transport, while the impacts of cross-inversion mixing dominate.

3.4 Sensitivity to Turbulent Mixing

In the NoTM experiment, turbulent mixing (TM) was "turned off". However, because TM is heavily responsible for transporting emitted dust upwards from the surface, TM is kept active ("turned on") over land (see Sect. 2.2). The NoTM experiment is therefore expected to have little to no change at the Sahara. Figure 9 shows size-resolved cross sections of mass concentration difference between the NoTM and Control simulations.

As expected, there is little to no change in mass concentration in any size bin over land (east of ∼ 17° W). Where there are slight changes, for example in size bins 1 and 4, these are likely to due to remixing of dust from over the ocean towards land. Removal of turbulent mixing over the ocean increases the mass concentration dust between 500 m to 2 km where TM would otherwise have been active in mixing dust down towards the ocean surface and very lowest layers of the atmosphere.

Three patterns in the response to removed TM over the ocean are visible in the six size bins. In size bin 1, there is an increase in mass concentration below 500 m of up to 0.006 $\mu g\,m^{-3}$, with a small decrease above this up to ∼ 1300 m. In size bins 2–4, the opposite pattern occurs: below 500 m, there is a decrease in mass concentration, with an increase above. Finally, in size bins 5 and 6, there is simply an increase in mass concentration which is strongest just west of the African coastline.

Despite appearing to have different reactions to removed TM, size bins 2–6 all show responses indicative of reduced mixing within the MBL. In size bins 2–4, the dust collects in the upper MBL, and is not mixed down to lower levels as it would be normally. Instead, without TM, the size bin 2–4 dust remains suspended within the upper MBL. However, the coarser size bins 5 and 6 are more strongly influenced by their greater gravitational settling velocity, depositing through the lower MBL to the surface. This change in mass vertical distribution in the MBL removes the sharp change in dust mass concentration usually present at the MBL-SAL interface, replacing it with a smooth gradient in concentration from the surface to the MBL-SAL interface (Fig. 5c, d).

Size bin 1 dust is particularly dependent on TM for deposition due to the small size and subsequently low mass re-

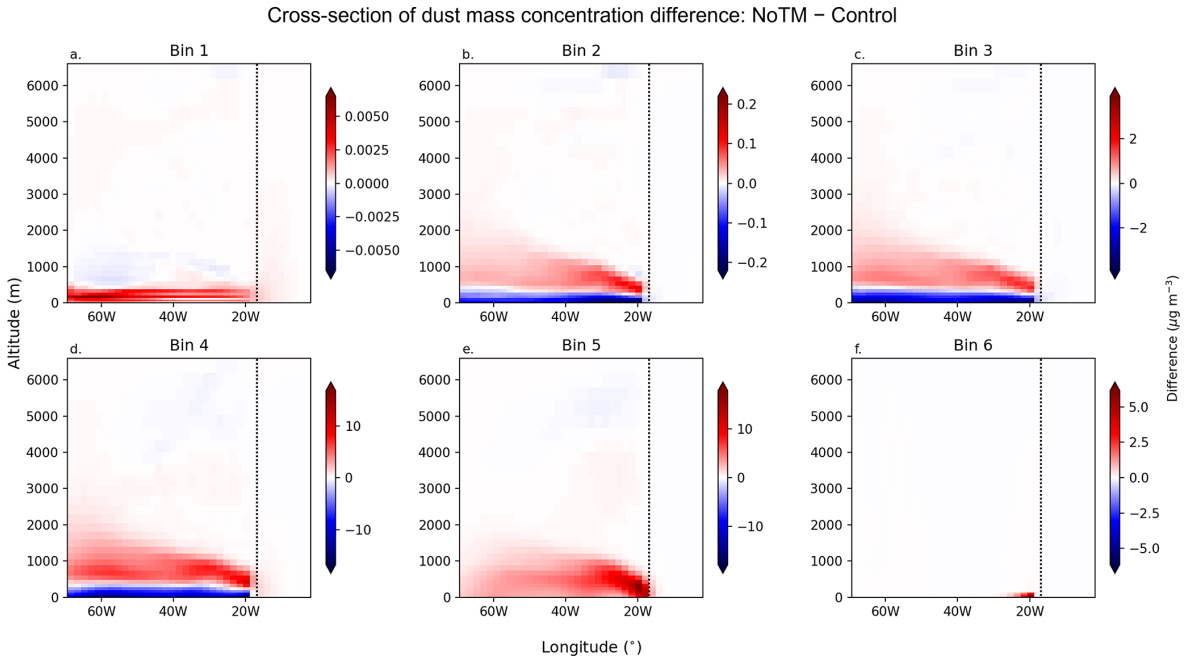

Figure 9. Impact of NoTM: Cross section of absolute difference of the size-resolved mass concentration in the NoTM and Control experiments. At 16.9° N, the cross sections span from 70° W to 0° E, and extend up to 6.5 km. The colour bar scale varies between each plot. The vertical dotted line approximately locates the west African coast.

sulting in little dependence on sedimentation. Thus without their main removal mechanism active, the size bin 1 particles concentrate in the lowest 500 m of the atmosphere (Fig. 9a) with few pathways to atmospheric removal available. This results in widespread, increased concentrations of size bin 1 particles over the North Atlantic (not shown), predominantly relying on wet deposition over land, and TM over land for removal. In removing TM, we reduced R_A and R_B to 0 in Eq. (3). R_B accounts in part for Brownian diffusion which is most dominant for particles with $d < 0.1$ µm. This may be why the impact on size bin 1 (0.0632–0.2 µm) is relatively unique to the other size bins.

All size bins show little to no change to mass concentration within the SAL suggesting that TM dominates mixing within the marine BL towards the surface. With distance from the Sahara, the vertical depth over which increases to mass concentration in size bins 2–5 occur grows upwards into the lower SAL. This suggests that there is some mixing of dust up into the SAL by convective mixing or diffusion from the upper MBL.

The NoTM experiment shows improved coarse particle (mainly size bin 5) transport to the west Atlantic, however, the changes to the vertical profile of dust result in a divergence of the model from the observed vertical dust profile (Fig. 5c, d). Thus, similar to the CM experiments, this experiment provides useful insight into the interaction of TM with dust in this climate model and its impact on vertical mixing within the MBL.

3.5 Sensitivity to Impaction scavenging

Removing IS from the model has the greatest impact at finer size ranges. Without IS, the concentration of fine dust particles increases in the atmosphere, in both the SAL and in the free troposphere. The NoIS experiment changes the vertical profile of total dust mass to the greatest degree of all the experiments, with large quantities of fine dust transported above the SAL, into the free troposphere (Fig. 5). Figure 4 shows the increased VSD of the four finest size bins, with more than one order of magnitude increase in size bin 1. At the coarse size range, the lack of IS also resulted in an increase of size bin 5 and 6 VSD. At Cape Verde (and the Caribbean), the size bin 5 VSD was 20 %–100 % (100 %–4000 %) greater and the size bin 6 VSD was 8 %–40 % (40 %–100 %) greater than in the Control. While this change is by no means insignificant, it lacks the magnitude required to bring this simulation into agreement with the observations. For example, the 0.2S simulation increased size bin 6 VSD by 1.6×10^7 % to bring the model up to the 10th percentile of observations seen during the SALTRACE campaign.

Despite the IS coefficient increasing broadly with size (as shown in Table 1), the impact of IS decreases with size. This is due to the impact of sedimentation increasing much more rapidly with size than the impact of IS, and thus, the sedimentation is so dominant for the coarsest size bins that changes to IS are negligible in comparison. Additionally, since IS is proportional to the dust mass concentration per size bin, IS removal will be weaker for the largest two size bins which

contain less mass in the model Control experiment. This also means IS will be strongest in the fine range, and we hypothesise that this is why IS is so important at the fine size range.

3.6 Sensitivity to Tripled SW Absorption

A large degree of uncertainty still exists in the size distribution and mineralogical composition of emitted mineral dust, which impacts the dust radiative effects. Li et al. (2021) and Di Biagio et al. (2020) suggest that the SW absorption of dust is often assumed to be too small and that increasing it can improve model meteorology (Balkanski et al., 2021). As suggested in the introduction (Sect. 1), the SW absorption of dust heats the atmosphere causing positive buoyancy, which can lead to upwards transport of aerosol, a process known as self-lofting, which could enhance coarse particle transport (Boers et al., 2010; Colarco et al., 2014; Johnson and Haywood, 2023; Khaykin et al., 2022). In order to test the impact of dust absorption on dust transport, we have tripled the SW absorption of dust in the model to force a significant response. This experiment requires dust to interact with radiation in the model, and therefore RE is turned on. This also results in altered meteorology and dust emissions (see Sect. 2.1.2). Therefore this experiment (3×SW) and a new control simulation (REControl) are not parallel to each other or the previous experiments. Analysis of the emissions from REControl and 3×SW over the 20 year modelled period showed that the two simulations have comparable dust emissions (not shown). Thus, while the comparison is not as robust as those carried out previously, the two simulations are assumed to be comparable within this study.

Figure 10 shows the normalised mean total dust mass concentration profiles from the REControl and 3×SW experiments and the aircraft campaigns, along with the MMA from the model simulations at the four analysed locations. At the Sahara, there is a greater mass loading in the 3×SW experiment compared to REControl from the surface up to ∼ 2 km altitude, lowering the MMA by ∼ 100 m. Though the profile averages are still within the standard deviation of each other. At the Canaries and Cape Verde, the two mean profiles are still within one standard deviation of each other, but show a slight increase in the MMA in the 3×SW experiment. After long-range transport at the Caribbean, the MMA in the 3×SW experiment is more than 500 m higher than the REControl MMA. Above ∼ 3.3 km, the profile standard deviations no longer overlap the other profiles mean, showing a more significant change in the vertical dust distribution. In the 3×SW experiment, the dust is transported at higher altitudes. Further analysis (not shown) has shown that the trans-Atlantic dust plume did not change location in terms of latitude significantly between the two experiments, suggesting that the changes shown in Fig. 10 are not a result of a horizontally shifted plume mass.

While Fig. 10 shows that the total dust mass is lofted higher after long-range transport, analysis of the size-resolved changes shows that the majority of change to mass loading is driven by size bins 2–4 (not shown). Between the two simulations, the two coarsest size bins show negligible difference at the Caribbean both in terms of the mass loading and vertical distribution. It is likely that the high sedimentation velocities of the largest particles are so large that they are not significantly counteracted by the additional upwards motion from SW absorption.

In the 3×SW experiment, there was an increase in air temperature of up to +1 K at the Sahara above 3 km altitude (Fig. S1 in the Supplement). In the east Atlantic, the SAL experiences greater heating in the 3×SW experiment, with a maximum increase of +0.9 K at ∼ 4 km altitude. At the Caribbean, air temperature was greater in the 3×SW experiment between 1.5–5 km altitude, with a peak of +0.7 K at 3.5 km altitude. These changes in air temperature are likely a direct result of the increased dust SW absorption influencing atmospheric heating rates.

In this experiment, absorption was specifically tripled to elicit a strong response, however, results show a relatively limited response of the dust. Colarco et al. (2014) tested the impact of different radiative properties of dust in a climate model. They found that their "most absorbing" representation of dust radiative properties brought their climate model (NASA GEOS-5; Goddard Earth Observing System Model, Version 5) into better agreement with observations, by increasing dust transport altitude, westwards dust transport, and atmospheric lifetime. Between their control experiment and with the "most absorbing" experiments, there was less difference in the dust radiative properties than between our REControl and 3×SW, yet the response of the changed dust properties appeared greater in their experiments than in our own. They attribute their findings to an enhanced longwave (LW) effect driven by including the representation of coarse particles (represented up to 10 µm diameter).

Compared to the 2001–2020 June mean AOD at 550 nm from MODIS Terra (Dark Target and Deep Blue combined; Fig. S2 in the Supplement), the 3×SW experiment has a lower mean AOD. The mean AOD in the box regions (Fig. 3) for the 3×SW model experiment (MODIS retrievals) are approximately 0.4 (0.5) at the Sahara, 0.1 (0.2) at the Canaries, 0.3 (0.7) at Cape Verde, and 0.1 (0.4) at the Caribbean. The relatively low AODs in the model will restrict the ability of the model to respond to dust-radiation interactions, and therefore may explain the limited impact of changing dust absorption in this work.

4 Discussion

In the HadGEM3-GA7.1 climate model, there are various processes which affect and determine the transport and deposition of mineral dust particles (represented in Fig. 1). These processes are often size-dependent, impacting the finest and coarsest particles in different ways. In order to dissect which

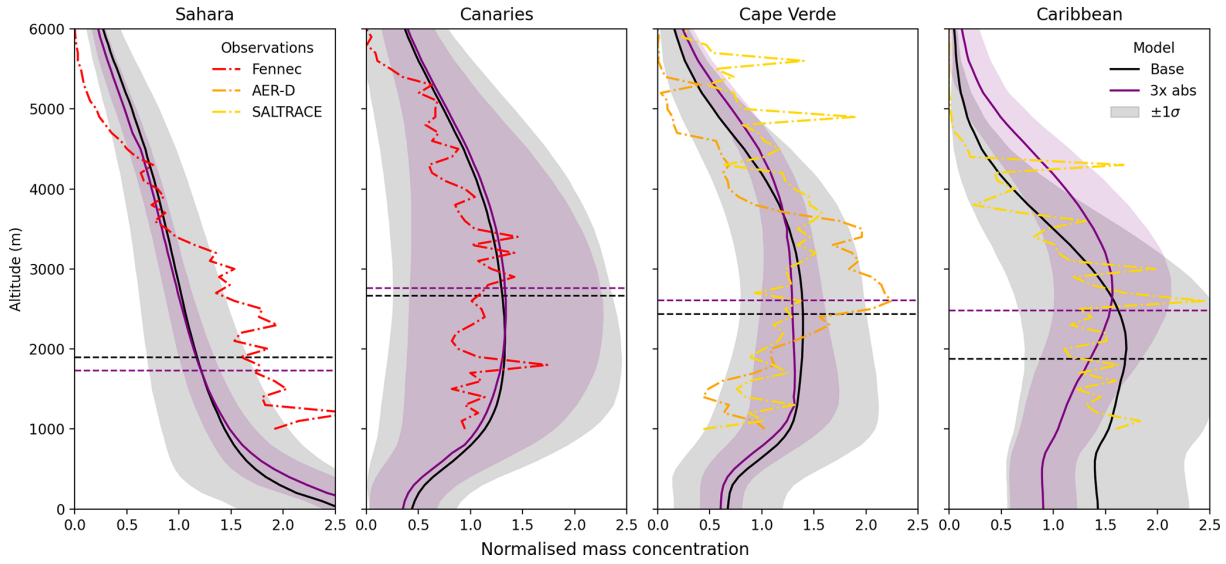

Figure 10. Normalised dust mass concentration profiles (0.0632–63.2 µm diameter) at the Sahara, Canaries, Cape Verde, and Caribbean in the REcontrol (black) and 3×SW (purple) simulations, and the aircraft campaigns (dot dash lines). The shading shows the standard deviation of the simulated profiles. The dashed lines represent the MMA of the model experiments between 0–6 km altitude. The MMA from the observations is not included due to the presence of non-dust aerosols in the MBL (below 1 km altitude) altering the value.

processes most dominantly impact the coarse particles in the model, we have run a series of experiments removing or scaling these processes.

We have shown that sedimentation has dominant control on the long-range transport of coarse particles in this model. Testing of the CM, TM, IS, and dust SW absorption has negligible impact on the long-range transport of coarse particles in the model. Sedimentation is the only process in the model which has both sufficient strength and size dependence that it can be adjusted to bring the model's coarse particle transport into agreement with observations. Reductions in sedimentation by 50 %–95 % are required in order to bring the model into better agreement with the observations in terms of the VSD. The required reduction in sedimentation increases with transport distance: from 50 %–80 % over the Sahara to 80 %–95 % at the Caribbean. The reductions to sedimentation also raise the altitude of the dust plume in the SAL, bringing it better into agreement with observations. The improvement of model dust size distribution following a significant reduction in sedimentation is not unique to HadGEM3-GA7.1. Drakaki et al. (2022) suggested a reduction of 40 %–80 % was required at the Sahara and East Atlantic in a simulation with the Weather Research and Forecasting model coupled with Chemistry (WRF-Chem). Also, Meng et al. (2022) showed that decreasing dust particle density by an order of magnitude and accounting for particle asphericity, resulting in a reduction of sedimentation velocity by 90 %–95 %, brought the Community Earth System Model (CESM) into agreement with observations in Saharan dust outflow regions. These studies cover varying grid resolution and model configurations; our study used a ∼ 190 km resolution global climate model, Drakaki et al. (2022) used a 15 km resolution NWP setup with a higher order advection scheme in the horizontal and vertical, and Meng et al. (2022) used a 190 km resolution global nudged climate simulation. Drakaki et al. (2022) and Meng et al. (2022) both employ an adaptation to Stokes law which is more representative for particles with an effective diameter greater than 10 µm, which may sit outside of the Stokes regime. Drakaki et al. (2022) use a drag coefficient suggested by Clift and Gauvin (1971), which is also used by Mallios et al. (2020) for representing prolate spheroids. With increasing size, the divergence between Stokes and the drag coefficient of Clift and Gauvin (1971) grows. Meng et al. (2022) use a Stokes correction factor which exceeds 10 % for particles with $d > 45$ µm (as described in Zender et al., 2003). Despite these differences in the model configurations, the results of this study and those of Drakaki et al. (2022) and Meng et al. (2022) suggesting order of magnitude reductions in settling velocity are required are remarkably similar. This suggests that model resolution (at least in super-km-scale modelling) is not the issue, and that despite differences in CM and TM parameterisations between the model's substantial changes to the sedimentation are required. As sedimentation is a well-understood process, we theorise that the reductions suggested here and elsewhere instead highlight an overarching issue in our understanding of the processes acting on coarse mineral dust particles in the atmosphere that are counteracting their sedimentation by 50 %–95 %. Our results are limited to the HadGEM3-GA7.1 model, so whilst we are not able to validate these results across models, which may use different atmospheric mixing and wet deposition schemes, we are able to see great similarity in the results

of the reduced sedimentation experiments with Drakaki et al. (2022) and Meng et al. (2022) across different models.

It should be noted that the sectional (i.e. use of size bins) representation of the dust size distribution could also contribute to the excessive loss of the dust in size bin 6 (20–62.3 µm). A sectional distribution is not able to represent the observed reduction in volume with increasing diameter within the range of size bin 6, so if the bin has the same total mass of dust as in the observations it will have too high a ratio of the largest to the smallest particles in that size bin and hence, a higher geometric mean diameter than observed, resulting in excessive sedimentation. Modal schemes are also not without their challenges, since the larger tails of the modal VSD are not able to adjust in the same way as shown by observations.

Mechanisms which are not represented in GCMs, such as electrical charging, particle asphericity, may be responsible for the counteraction of coarse particle sedimentation in the real-world, however, it is still not fully understood how much of an impact these mechanisms play. The results of this work re-emphasize the importance of improving our understanding of these processes, since reductions to sedimentation were the only changes resulting in the necessary retention of coarse dust. Huang et al. (2020) estimate the impact of asphericity could increase coarse particle lifetime by ∼ 20 %, though this assumes that the particles are randomly oriented. In a scenario where the particles are horizontally oriented in the atmosphere they would experience increased drag, and subsequently increased lifetime (Mallios et al., 2020). However, at deposition buoys across the Atlantic, van der Does et al. (2018) found particles over 200 µm diameter were individual spherical quartz particles. In this case, this would suggest alternative mechanisms had resulted in the long-range transport, for example, electrical charging, which may transport particles at a greater altitude (Toth et al., 2020) and over greater distances (Méndez Harper et al., 2022). Electrical charge may be retained for longer on rounder, more spherical particles, rather than aspherical ones which are more likely to experience charge accumulation and discharge in the narrower tips (which Griffiths and Latham, 1974 found experimentally in ice crystals). Additionally, quartz particles are found experimentally to experience greater charging than clay minerals (Harrison et al., 2016, and references therein). It is hypothesised that charging of aspherical particles could result in orientation of the particles with the longest axis positioned vertically (Ulanowski et al., 2007). It is not fully understood how the effects of asphericity and electrical charging interact with each other to alter coarse particle lifetime.

This study is the first time, to our knowledge, that all the processes in a model impacting the coarse particle lifetime have been tested, with previous studies only focusing on the gravitational settling velocity. The overarching impact of CM, TM and gravitational settling on vertical movements of dust in the model are shown in a schematic alongside the resulting impact of the NoCM and NoTM experiments

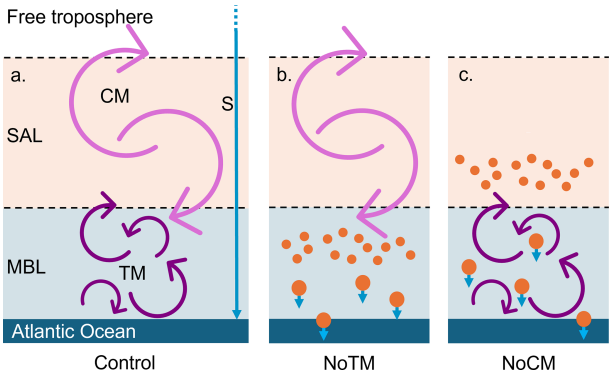

Figure 11. Schematic showing the simplified vertical extent of convective mixing (CM; pink), turbulent mixing (TM; purple), and sedimentation (S; blue) in the model over the Atlantic Ocean **(a)**. Additionally, the resultant clustering of finer dust (size bins 2–4) in the NoTM **(b)** and NoCM **(c)** experiments is shown. The depth of the MBL is approximately 1 km, and the height of the SAL top is between 4–6 km.

(Fig. 11). The first panel (Fig. 11a) shows an approximation of the ranges in which TM, CM, and sedimentation act within the atmosphere in the Control simulation. TM acts within the MBL, CM acts within the SAL and across its upper and lower boundaries, while sedimentation is present throughout the depth of the atmosphere. In the NoTM experiment (Fig. 11b), reduced mixing within the MBL resulted in excessive finer dust mass (size bins 2–4) collecting in the upper MBL, preventing mixing down to the surface. The continued presence of CM in the SAL in the NoTM experiment, resulted in normal concentrations and vertical distribution of dust within the SAL and free troposphere. Coarse particles (size bins 5 and 6) with their greater mass, were still most influenced by sedimentation, and continued to deposit through the lower MBL to the surface. However, in the NoCM experiment (Fig. 11c), the removal of CM had a dominant impact on the vertical distribution within the SAL of the finer dust, resulting in higher concentrations of finer dust collecting in the lower SAL, reducing mixing down into the MBL. Sedimentation dominates the vertical transport of the coarse particles, continuing to mix them across the SAL-MBL inversion downwards towards the surface.

While neither the NoTM or NoCM experiments had a great enough impact on the long-range transport of coarse dust mass to reach agreement with observations, we have shown the importance of the mixing mechanisms for maintaining and governing the modelled vertical distribution of dust. The experiments carried out in this paper show that the finer, lighter particles are more subject to CM, TM and IS that the coarse particles, which are dominantly governed by sedimentation. The simulations did show that the larger (size bin 5–6) dust particles respond to CM changes over the Sahara within and above the SABL. For example, in the doubled CM experiment, dust in these size bins underwent enhanced

vertical transport to above the SABL, although the absolute changes in mass were very small, probably as a result of the dominant effects of sedimentation. However, it does demonstrate the importance of CM in governing coarse dust vertical transport, and could have stronger impacts if sedimentation were not so strong. Additionally, a more moderate adjustment of increase to CM (rather than a doubling) may have resulted in a better representation of coarse dust higher up in the SABL, rather than causing it to be mixed (unrealistically) into the free atmosphere above the SABL. Removing TM from the model did result in some additional size bin 5 transport towards the Caribbean in the MBL as they are not mixed down to the surface. This does not directly explain the presence of coarse particles in the SAL measured by the AER-D and SALTRACE campaigns, but this may suggest that TM could be acting too strongly in mixing dust down towards the surface.

Rodakoviski et al. (2023) found that a LES of a turbulent shear layer was capable of improving the lifetime of coarse, aspherical dust particles enough to result in long-range transport. This finding suggests that the representation of TM within a model may be key to better representations of coarse particle long-range transport. Rodakoviski et al. (2023) represent turbulent motions within the SAL, whereas TM in HadGEM3-GA7.1 is represented mainly in the MBL, below the SAL, meaning that the majority of dust in the modelled SAL is not under the influence of turbulent motions.

The higher dust particles are transported vertically upwards through the SABL, the longer their atmospheric lifetime is expected to be. Firstly there is a larger altitude range to overcome in order for deposition to occur, and secondly dust is more likely to transported to parts of the atmosphere with stronger horizontal wind speeds (typically the African easterly jet, peaking at around 700 hPa, with wind speeds up to 25 $\mathrm{m\,s^{-1}}$; Chouza et al., 2016), enabling faster westwards transport. This is part of the hypothesis behind our CM experiments; increased CM at the Sahara could transport dust particles higher. However, if there is something inherent in the model which inhibits this initial vertical mixing, the long-range transport of coarse particles will still be limited. An additional experiment (not shown here) tested the importance of particle injection height at the Sahara by injecting the model dust directly at 5 km altitude above the Sahara. We found that the time taken for 50 % of size bin 6 dust (20–63.2 µm) to be deposited increased from ~ 3 to ~ 12 h when the dust was raised (Fig. S3 in the Supplement). Transport time from the west coast of Africa to Barbados is expected to take 5 d or within the range of 120 h (Chouza et al., 2016). Therefore we conclude that sedimentation for super-coarse dust still dominates the transport and deposition processes in the model, even when dust is artificially injected high up in the SABL.

Whereas in this study we only tested one process at a time, there is scope for future work to test the sensitivity of coarse particle transport to a combination of these processes. Additional testing could include combining the effects of reduced sedimentation with altered TM and CM in the SAL, or with increased SW absorption, which showed evidence of improved coarse particle vertical distribution. Since all the sensitivity experiments tested here showed some impacts on dust transport which were size-dependent, it would be useful for further work to investigate combined sensitivity tests. For example, a moderate reduction to sedimentation could be implemented (such as 0.5S) and combined with other dust transport adjustments. This would result in increased retention of dust in size bins 5–6, which should then enable the other altered processes to impact the coarse dust VSD evolution. This could then allow, for example, IS to increase dust VSD across the full size range, 2×CM to increase coarse dust within and above the SABL at more significant mass concentrations, or 3×SW to have a more significant effect due to the more absorbing nature of coarse dust. Additionally, testing the reduction of sedimentation of only the two coarsest size bins could be beneficial. Further theoretical and observational work to better understand how reduced sedimentation due to other processes, such as electrical charging or particle asphericity, may impact different dust size ranges, would be beneficial here in informing further experiments.

5 Conclusions

In this study, we conducted a series of climate model experiments to increase understanding of processes that impact the transport and deposition of coarse mineral dust particles, which models fail to represent. A series of 20-year sensitivity tests are run using the HadGEM3-GA7.1 climate configuration from the Met Office Unified Model. These experiments, testing sedimentation, convective mixing (CM), turbulent mixing (TM), impaction scavenging, and dust shortwave (SW) absorption, reveal important information about the role these processes play in determining the transport and distribution of mineral dust particles in the model. To our knowledge, this is the first time a study has tested all the processes impacting the dust transport and deposition in a model.

We have shown that sedimentation is the only process capable of making the multi-order of magnitude changes required to bring the model into agreement with observations in terms of coarse dust long-range transport. All other tested processes were found to have minimal impact on coarse particle transport, but did reveal insights on the vertical mixing and fine particle transport. Reducing sedimentation results in coarse particles being transported further and at higher altitudes. In order to improve the coarse particle size distribution over long-range transport, a reduction of 50 %–80 % reconciles the modelled dust size distribution with observations at the Sahara, but in order to match observations at the Caribbean, a reduction of 80 %–95 % was required. Sedimentation is a well-understood process, hence, we the-

orise an overarching issue exists in our understanding of the processes acting on coarse mineral dust particles in the atmosphere which is counteracting their sedimentation by ∼ 50 %–95 %. Processes not considered in the model and/or not well understood in general may be the root cause of recurring underestimations of coarse particle long-range transport. There are a few mechanisms which are speculated to increase coarse particle transport, but are not typically represented in GCMs (i.e. particle asphericity and electrical charging). Future work should include using theoretical and observational work to better understand how these processes impact coarse particle transport, but also how they may interact.

Impaction scavenging was found to be more important for the removal of fine particles due to the overarching dominance of sedimentation in controlling the deposition of coarse particles. We found that tripling SW absorption, despite being a large and unrealistic change, did not greatly impact the concentration of coarse particles retained in long-range transport. We found that by tripling SW absorption of dust, the air temperature was raised by up to 1 K over the Sahara and within the SAL, and that the total dust mass was carried up to 500 m higher in the atmosphere.

TM and CM have been shown here to be important in controlling the vertical distribution of dust in the model marine boundary layer (MBL), Saharan air layer (SAL), and Saharan atmospheric boundary layer (SABL). CM controls the vertical distribution of dust within the SAL and SABL and the mixing of dust out of them (both above, below and horizontally); without CM, the dust concentration in the lower SAL increases. Doubled CM reduced coarse dust mass in the lowest parts of the SABL and increased mixing from the SABL into the free atmosphere above. TM controls the vertical distribution of dust primarily within the MBL, mixing dust downward through the depth of the MBL towards the surface, and governing the deposition of the finer particles to the surface. Without TM, dust collects in the upper MBL, less readily mixed down through the lowest 500 m of the atmosphere. The coarse particles with their larger mass still have great enough sedimentation to be relatively insensitive to CM and TM changes, and settle through the SAL and MBL regardless.

In this study, we use the HadGEM3-GA7.1 model configuration with a tuned emitted dust size distribution that emits more coarse particles than the standard tuning used in the HadGEM3-GA7.1 CMIP6 setup. We have shown that despite improving the emissions, the divergence of the modelled transported size distribution is exacerbated with transport. Thus, while emissions are an important factor in dust modelling, a bias in dust size distribution develops during transport which cannot be improved with tuning and improved emissions alone.

Through a series of sensitivity studies in a climate model, we have shown that reducing sedimentation is the most efficient way to bring the long-range transport of coarse particles in the model into agreement with in-situ aircraft observations. This work confirms the presence of one or more processes counteracting the sedimentation of coarse particles by a compelling 50 %–95 %. Though we have a better understanding of the magnitude of the counteraction, the nature of these processes remains poorly understood and explored. In order to diagnose these processes, we suggest future research into model representations of mechanisms altering coarse particle lifetime, such as asphericity, electrical charging, TM, and tests to better understand how higher grid resolution can change model processes such as TM and CM, including how these processes might interact with a reduction in sedimentation, which consequently impact dust transport, as well as observational studies to understand these processes.

Code and data availability. Due to intellectual property rights restrictions, we cannot provide either the source code or documentation papers for the UM. The Met Office Unified Model is available for use under licence. A number of research organisations and national meteorological services use the UM in collaboration with the Met Office to undertake basic atmospheric process research, produce forecasts, develop the UM code, and build and evaluate Earth system models. For further information on how to apply for a licence, see https://www.metoffice.gov.uk/research/approach/modelling-systems/unified-model (Met Office, 2026).

Aircraft data for the Fennec and AER-D campaigns are available at the Center for Environmental Data Archive at https://doi.org/10.5285/1f4555d2589841a8a4bbbf1fe42f54c8 (Facility for Airborne Atmospheric Measurements et al., 2018) and http://catalogue.ceda.ac.uk/uuid/d7e02c75191a4515a28a208c8a069e70 (Facility for Airborne Atmospheric Measurements and Blyth, 2015), respectively. Aircraft data for the SALTRACE campaign is currently in the process having a DOI created. Data from the model simulations are in the process of having a DOI created.

Supplement. The supplement related to this article is available online at https://doi.org/10.5194/acp-26-16779-2026-supplement.

Author contributions. NGR, CLR, NB, SW, AJ, and BJ designed the research, discussed the methodology and results. NGR carried out the analysis and wrote the paper. BW, LMW and JG provided the SALTRACE data. All authors read and commented on the paper.

Competing interests. The contact author has declared that none of the authors has any competing interests.

Disclaimer. Publisher's note: Copernicus Publications remains neutral with regard to jurisdictional claims made in the text, published maps, institutional affiliations, or any other geographical representation in this paper. The authors bear the ultimate responsibility for providing appropriate place names. Views expressed in the text are those of the authors and do not necessarily reflect the views of the publisher.

Acknowledgements. NGR would like to acknowledge the funding and support given by CASE funding from the UK Met Office. NGR acknowledges the use of the MONSooN system, a collaborative facility supplied under the Joint Weather and Climate Research Programme, a strategic partnership between the Met Office and the Natural Environment Research Council. LMW and BW acknowledge funding through the University of Vienna and the Gottfried-and-Vera Weiss Foundation and FWF in the context of the PlasticSphere project (AP3641721).

Financial support. This research has been supported by the Natural Environment Research Council (grant nos. NE/S007261/1 and NE/M018288/1).

Review statement. This paper was edited by N'Datchoh Evelyne Touré and reviewed by two anonymous referees.

References

Adebiyi, A., Kok, J. F., Murray, B. J., Ryder, C. L., Stuut, J.-B. W., Kahn, R. A., Knippertz, P., Formenti, P., Mahowald, N. M., García-Pando, C. P., Klose, M., Ansmann, A., Samset, B. H., Ito, A., Balkanski, Y., Di Biagio, C., Romanias, M. N., Huang, Y., and Meng, J.: A review of coarse mineral dust in the Earth system, Aeolian Res., 60, 100849, https://doi.org/10.1016/j.aeolia.2022.100849, 2023.

Adebiyi, A. A. and Kok, J. F.: Climate models miss most of the coarse dust in the atmosphere, Sci. Adv., 6, https://doi.org/10.1126/sciadv.aaz9507, 2020.

Alfaro, S. C. and Gomes, L.: Modeling mineral aerosol production by wind erosion: Emission intensities and aerosol size distributions in source areas, J. Geophys. Res.-Atmos., 106, 18075–18084, https://doi.org/10.1029/2000JD900339, 2001.

Bagnold, R. A.: The Physics of Blown Sand and Desert Dunes, Metheun, New York, ISBN 978-94-009-5682-7, 1941.

Balkanski, Y., Schulz, M., Claquin, T., and Guibert, S.: Reevaluation of Mineral aerosol radiative forcings suggests a better agreement with satellite and AERONET data, Atmos. Chem. Phys., 7, 81–95, https://doi.org/10.5194/acp-7-81-2007, 2007.

Balkanski, Y., Bonnet, R., Boucher, O., Checa-Garcia, R., and Servonnat, J.: Better representation of dust can improve climate models with too weak an African monsoon, Atmos. Chem. Phys., 21, 11423–11435, https://doi.org/10.5194/acp-21-11423-2021, 2021.

Bellouin, N., Rae, J., Jones, A., Johnson, C., Haywood, J., and Boucher, O.: Aerosol forcing in the Climate Model Intercomparison Project (CMIP5) simulations by HadGEM2-ES and the role of ammonium nitrate, J. Geophys. Res.-Atmos., 116, https://doi.org/10.1029/2011JD016074, 2011.

Betzer, P., Carder, K., Duce, R., Merrill, J., Tindale, N., Uematsu, M., Costello, D., Young, R., Feely, R., Breland, J., Bernstein, R., and Greco, A.: Long–range transport of giant mineral aerosol particles, Nature, 336, 568–571, https://doi.org/10.1038/336568a0, 1988.

Boers, R., de Laat, A. T., Stein Zweers, D. C., and Dirksen, R. J.: Lifting potential of solar-heated aerosol layers, Geophys. Res. Lett., 37, https://doi.org/10.1029/2010GL045171, 2010.

Brown, A. R., Beare, R. J., Edwards, J. M., Lock, A. P., Keogh, S. J., Milton, S. F., and Walters, D. N.: Upgrades to the boundary-layer scheme in the Met Office numerical weather prediction model, Bound.-Lay. Meteorol., 128, 117–132, 2008.

Carlson, T. N.: The Saharan Elevated Mixed Layer and its Aerosol Optical Depth, The Open Atmospheric Science Journal, 10, 26–38, https://doi.org/10.2174/1874282301610010026, 2016.

Checa-Garcia, R., Balkanski, Y., Albani, S., Bergman, T., Carslaw, K., Cozic, A., Dearden, C., Marticorena, B., Michou, M., van Noije, T., Nabat, P., O'Connor, F. M., Olivié, D., Prospero, J. M., Le Sager, P., Schulz, M., and Scott, C.: Evaluation of natural aerosols in CRESCENDO Earth system models (ESMs): mineral dust, Atmos. Chem. Phys., 21, 10295–10335, https://doi.org/10.5194/acp-21-10295-2021, 2021.

Chouza, F., Reitebuch, O., Benedetti, A., and Weinzierl, B.: Saharan dust long-range transport across the Atlantic studied by an airborne Doppler wind lidar and the MACC model, Atmos. Chem. Phys., 16, 11581–11600, https://doi.org/10.5194/acp-16-11581-2016, 2016.

Clift, R. and Gauvin, W. H.: Motion of entrained particles in gas streams, Can. J. Chem. Eng., 49, 439–448, https://doi.org/10.1002/cjce.5450490403, 1971.

Colarco, P. R., Nowottnick, E. P., Randles, C. A., Yi, B., Yang, P., Kim, K. M., Smith, J. A., and Bardeen, C. G.: Impact of radiatively interactive dust aerosols in the NASA GEOS-5 climate model: Sensitivity to dust particle shape and refractive index, J. Geophys. Res., 119, 753–786, https://doi.org/10.1002/2013JD020046, 2014.

Cornwell, G. C., Xiao, H., Berg, L. K., and Burrows, S. M.: Simulated dust transport in the convective boundary layer, J. Geophys. Res.-Atmos., 126, https://doi.org/10.1029/2020jd033429, 2021.

Cuesta, J., Marsham, J. H., Parker, D. J., and Flamant, C.: Dynamical mechanisms controlling the vertical redistribution of dust and the thermodynamic structure of the West Saharan atmospheric boundary layer during summer, Atmos. Sci. Lett., 10, 34–42, https://doi.org/10.1002/asl.207, 2009.

Denjean, C., Cassola, F., Mazzino, A., Triquet, S., Chevaillier, S., Grand, N., Bourrianne, T., Momboisse, G., Sellegri, K., Schwarzenbock, A., Freney, E., Mallet, M., and Formenti, P.: Size distribution and optical properties of mineral dust aerosols transported in the western Mediterranean, Atmos. Chem. Phys., 16, 1081–1104, https://doi.org/10.5194/acp-16-1081-2016, 2016.

Di Biagio, C., Balkanski, Y., Albani, S., Boucher, O., and Formenti, P.: Direct Radiative Effect by Mineral Dust Aerosols Constrained by New Microphysical and Spectral Optical Data, Geophys. Res. Lett., 47, 1–12, https://doi.org/10.1029/2019GL086186, 2020.

Drakaki, E., Amiridis, V., Tsekeri, A., Gkikas, A., Proestakis, E., Mallios, S., Solomos, S., Spyrou, C., Marinou, E., Ryder, C. L., Bouris, D., and Katsafados, P.: Modeling coarse and giant desert dust particles, Atmos. Chem. Phys., 22, 12727–12748, https://doi.org/10.5194/acp-22-12727-2022, 2022.

Evan, A. T., Flamant, C., Fiedler, S., and Doherty, O.: An analysis of aeolian dust in climate models, Geophys. Res. Lett., 41, 5996–6001, https://doi.org/10.1002/2014GL060545, 2014.

Facility for Airborne Atmospheric Measurements and Blyth, A.: UK ICE-D: atmospheric measurements dataset collection, Centre for Environmental Data Analysis [data set], http://catalogue.ceda.ac.uk/uuid/d7e02c75191a4515a28a208c8a069e70 (last access: 20 November 2026), 2015.

Facility for Airborne Atmospheric Measurements, Natural Environment Research Council, and Met Office: FAAM B606 FENNEC, LADUNEX and EUFAR flight: Airborne atmospheric measurements from core and non-core instrument suites on board the BAE-146 aircraft, NCAS British Atmospheric Data Centre [data set], https://doi.org/10.5285/1f4555d2589841a8a4bbbf1fe42f54c8, 2018.

Fécan, F., Marticorena, B., and Bergametti, G.: Parametrization of the increase of the aeolian erosion threshold wind friction velocity due to soil moisture for arid and semi-arid areas, Ann. Geophys., 17, 149–157, https://doi.org/10.1007/s00585-999-0149-7, 1999.

Gasteiger, J., Groß, S., Sauer, D., Haarig, M., Ansmann, A., and Weinzierl, B.: Particle settling and vertical mixing in the Saharan Air Layer as seen from an integrated model, lidar, and in situ perspective, Atmos. Chem. Phys., 17, 297–311, https://doi.org/10.5194/acp-17-297-2017, 2017.

Gillette, D. A.: Environmental factors affecting dust emission by wind erosion, in: Saharan Dust, John Wiley, New York, ISBN 9780471996804, 1979.

Gliß, J., Mortier, A., Schulz, M., Andrews, E., Balkanski, Y., Bauer, S. E., Benedictow, A. M. K., Bian, H., Checa-Garcia, R., Chin, M., Ginoux, P., Griesfeller, J. J., Heckel, A., Kipling, Z., Kirkevåg, A., Kokkola, H., Laj, P., Le Sager, P., Lund, M. T., Lund Myhre, C., Matsui, H., Myhre, G., Neubauer, D., van Noije, T., North, P., Olivié, D. J. L., Rémy, S., Sogacheva, L., Takemura, T., Tsigaridis, K., and Tsyro, S. G.: AeroCom phase III multi-model evaluation of the aerosol life cycle and optical properties using ground- and space-based remote sensing as well as surface in situ observations, Atmos. Chem. Phys., 21, 87–128, https://doi.org/10.5194/acp-21-87-2021, 2021.

Gregory, D. and Allen, S.: The effect of convective downdraughts upon NWP and climate simulations, in: Nineth conference on numerical weather prediction, 122–123, CRiD: 1573387449062676096, https://cir.nii.ac.jp/crid/1573387449062676096 (last access: 20 November 2026), 1991.

Gregory, D. and Rowntree, P. R.: A massflux convection scheme with representation of cloud ensemble characteristics and stability dependent closure, Mon. Weather Rev., 118, 1483–1506, https://doi.org/10.1175/1520-0493(1990)118<1483:AMFCSW>2.0.CO;2, 1990.

Griffiths, R. F. and Latham, J.: Electrical corona from ice hydrometeors, Q. J. Roy. Meteor. Soc., 100, 163–180, https://doi.org/10.1002/qj.49710042404, 1974.

Harrison, R. G., Barth, E., Esposito, F., Merrison, J., Montmessin, F., Aplin, K. L., Borlina, C., Berthelier, J. J., Déprez, G., Farrell, W. M., Houghton, I. M. P., Renno, N. O., Nicoll, K. A., Tripathi, S. N., and Zimmerman, M.: Applications of Electrified Dust and Dust Devil Electrodynamics to Martian Atmospheric Electricity, Space Sci. Rev., 203, 299–345, https://doi.org/10.1007/s11214-016-0241-8, 2016.

Harrison, R. G., Nicoll, K. A., Marlton, G. J., Ryder, C. L., and Bennett, A. J.: Saharan dust plume charging observed over the UK, Environ. Res. Lett., 13, https://doi.org/10.1088/1748-9326/aabcd9, 2018.

Heisel, M., Chen, B., Kok, J. F., and Chamecki, M.: Gentle Topography Increases Vertical Transport of Coarse Dust by Orders of Magnitude, J. Geophys. Res.-Atmos., 126, https://doi.org/10.1029/2021JD034564, 2021.

Holben, B. N., Tanre, D., Smirnov, A., Eck, T. F., Slutsker, I., Abuhassan, N., Newcomb, W. W., Schafer, J., Chatenet, B., Lavenue, F., Kaufman, Y. J., Castle, J. V., Setzer, A., Markham, B., Clark, D., Frouin, R., Halthore, R., Karnieli, A., O'Neill, N. T., Pietras, C., Pinker, R. T., Voss, K., and Zibordi, G.: An emerging ground-based aerosol climatology: Aerosol Optical Depth from AERONET, J. Geophys. Res., 106, 12067–12097, https://doi.org/10.1029/2001JD900014, 2001.

Huang, Y., Kok, J. F., Kandler, K., Lindqvist, H., Nousiainen, T., Sakai, T., Adebiyi, A., and Jokinen, O.: Climate models and remote sensing retrievals neglect substantial desert dust asphericity, Geophys. Res. Lett., 47, https://doi.org/10.1029/2019GL086592, 2020.

Johnson, B. T. and Haywood, J. M.: Assessing the Impact of Self-Lofting on Increasing the Altitude of Black Carbon in a Global Climate Model, J. Geophys. Res.-Atmos., 128, e2022JD038039, https://doi.org/10.1029/2022JD038039, 2023.

Jones, A. C., Hill, A., Hemmings, J., Lemaitre, P., Quérel, A., Ryder, C. L., and Woodward, S.: Below-cloud scavenging of aerosol by rain: a review of numerical modelling approaches and sensitivity simulations with mineral dust in the Met Office's Unified Model, Atmos. Chem. Phys., 22, 11381–11407, https://doi.org/10.5194/acp-22-11381-2022, 2022.

Karydis, V. A., Kumar, P., Barahona, D., Sokolik, I. N., and Nenes, A.: On the effect of dust particles on global cloud condensation nuclei and cloud droplet number, J. Geophys. Res.-Atmos., 116, https://doi.org/10.1029/2011JD016283, 2011.

Khaykin, S. M., de Laat, A. T. J., Godin-Beekmann, S., Hauchecorne, A., and Ratynski, M.: Unexpected self-lofting and dynamical confinement of volcanic plumes: the Raikoke 2019 case, Sci. Rep., 12, https://doi.org/10.1038/s41598-022-27021-0, 2022.

Kok, J. F.: Does the size distribution of mineral dust aerosols depend on the wind speed at emission?, Atmos. Chem. Phys., 11, 10149–10156, https://doi.org/10.5194/acp-11-10149-2011, 2011.

Kok, J. F., Ridley, D. A., Miller, R. L., Zhao, C., Heald, C. L., Ward, D. S., Albani, S., and Haustein, K.: Smaller desert dust cooling effect estimated from analysis of dust size and abundance, Nat. Geosci., 10, 274–278, https://doi.org/10.1038/ngeo2912, 2017.

Kok, J. F., Storelvmo, T., Karydis, V. A., Adebiyi, A. A., Mahowald, N. M., Evan, A. T., He, C., and Leung, D. M.: Mineral dust aerosol impacts on global climate and climate change, Nat. Rev. Earth Environ., 1–16, https://doi.org/10.1038/s43017-022-00379-5, 2023.

Kok, J. F., Gupta, A. K., Evan, A. T., García-Pando, C. P., Li, L., Adebiyi, A. A., Albani, S., Balkanski, Y., Checa-Garcia, R., Colarco, P. R., Hamilton, D. S., Huang, Y., Ito, A., Klose, M., Mahowald, N. M., Miller, R. L., Obiso, V., Lima, A. R., and Wan, J.: Desert dust exerts twice the longwave radiative heating estimated by climate models, Nat. Commun., 17, https://doi.org/10.1038/s41467-026-70952-9, 2026.

Kotsyfakis, M., Zarogiannis, S. G., and Patelarou, E.: The Health Impact of Saharan Dust Exposure, Int. J. Occup. Med. Env., 32, https://doi.org/10.13075/ijomeh.1896.01466, 2019.

Laakso, L., onholm, T. G., Rannik, U., Kosmale, M., Fiedler, V., aki, H. V., and Kulmala, M.: Ultrafine particle scavenging coefficients calculated from 6 years field measurements, Atmos. Environ., 37, 3605–3613, https://doi.org/10.1016/S1352-2310(03)00326-1, 2003.

Levy, R. C., Mattoo, S., Munchak, L. A., Remer, L. A., Sayer, A. M., Patadia, F., and Hsu, N. C.: The Collection 6 MODIS aerosol products over land and ocean, Atmos. Meas. Tech., 6, 2989–3034, https://doi.org/10.5194/amt-6-2989-2013, 2013.

Li, L., Mahowald, N. M., Miller, R. L., Pérez García-Pando, C., Klose, M., Hamilton, D. S., Gonçalves Ageitos, M., Ginoux, P., Balkanski, Y., Green, R. O., Kalashnikova, O., Kok, J. F., Obiso, V., Paynter, D., and Thompson, D. R.: Quantifying the range of the dust direct radiative effect due to source mineralogy uncertainty, Atmos. Chem. Phys., 21, 3973–4005, https://doi.org/10.5194/acp-21-3973-2021, 2021.

Lock, A. P.: The numerical representation of entrainment in parametrizations of boundary layer turbulent mixing, Mon. Weather Rev., 129, 1148–1163, 2001.

Lock, A. P., Brown, A. R., Bush, M. R., Martin, G. M., and Smith, R. N. B.: A new boundary layer mixing scheme. Part I: Scheme description and single-column model tests, Mon. Weather Rev., 128, 3187–3199, 2000.

Lu, Z., Wang, J., Chen, X., Zeng, J., Wang, Y., Xu, X., Christian, K. E., Yorks, J. E., Nowottnick, E. P., Reid, J. S., and Xian, P.: First Mapping of Monthly and Diurnal Climatology of Saharan Dust Layer Height Over the Atlantic Ocean From EPIC/DSCOVR in Deep Space, Geophys. Res. Lett., 50, https://doi.org/10.1029/2022GL102552, 2023.

Mallios, S. A., Drakaki, E., and Amiridis, V.: Effects of dust particle sphericity and orientation on their gravitational settling in the earth's atmosphere, J. Aerosol Sci., 150, https://doi.org/10.1016/j.jaerosci.2020.105634, 2020.

Marcotte, A. R., Anbar, A. D., Majestic, B. J., and Herckes, P.: Mineral Dust and Iron Solubility: Effects of Composition, Particle Size, and Surface Area, Atmosphere, 11, https://doi.org/10.3390/atmos11050533, 2020.

Marticorena, B. and Bergametti, G.: Modeling the atmospheric dust cycle: 1. Design of a soil-derived dust emission scheme, J. Geophys. Res., 100, 415–431, https://doi.org/10.1029/95JD00690, 1995.

Méndez Harper, J., Harvey, D., Huang, T., McGrath, J., Meer, D., and Burton, J. C.: The lifetime of charged dust in the atmosphere, PNAS Nexus, 1, https://doi.org/10.1093/pnasnexus/pgac220, 2022.

Meng, J., Huang, Y., Leung, D. M., Li, L., Adebiyi, A. A., Ryder, C. L., Mahowald, N. M., and Kok, J. F.: Improved Parameterization for the Size Distribution of Emitted Dust Aerosols Reduces Model Underestimation of Super Coarse Dust, Geophys. Res. Lett., 49, https://doi.org/10.1029/2021GL097287, 2022.

Met Office: Unified Model, https://www.metoffice.gov.uk/research/approach/modelling-systems/unified-model (last access: 11 September 2025), 2026.

Nachtergaele, F., van Velthuizen, H., Verelst, L., Batjes, N., Dijkshoorn, K., van Engelen, V., Fischer, G., Jones, A., Montanarella, L., Petri, M., Prieler, S., Teixeira, E., Wiberg, D., and Shi, X.: Harmonized World Soil Database (version 1.0), FAO, Rome, Italy and IIASA, Laxenburg, Austria, https://edepot.wur.nl/30776 (last access: 22 May 2026), 2008.

Nicoll, K., Harrison, G., Marlton, G., and Airey, M.: Consistent dust electrification from Arabian Gulf sea breezes, Environ. Res. Lett., 15, 084050, https://doi.org/10.1088/1748-9326/ab9e20, 2020.

Nicoll, K. A., Harrison, R. G., and Ulanowski, Z.: Observations of Saharan dust layer electrification, Environ. Res. Lett., 6, 014001, https://doi.org/10.1088/1748-9326/6/1/014001, 2011.

O'Sullivan, D., Marenco, F., Ryder, C. L., Pradhan, Y., Kipling, Z., Johnson, B., Benedetti, A., Brooks, M., McGill, M., Yorks, J., and Selmer, P.: Models transport Saharan dust too low in the atmosphere: a comparison of the MetUM and CAMS forecasts with observations, Atmos. Chem. Phys., 20, 12955–12982, https://doi.org/10.5194/acp-20-12955-2020, 2020.

Otto, S., Trautmann, T., and Wendisch, M.: On realistic size equivalence and shape of spheroidal Saharan mineral dust particles applied in solar and thermal radiative transfer calculations, Atmos. Chem. Phys., 11, 4469–4490, https://doi.org/10.5194/acp-11-4469-2011, 2011.

Prospero, J. M., Landing, W. M., and Schulz, M.: African dust deposition to Florida: Temporal and spatial variability and comparisons to models, J. Geophys. Res., 115, D13304, https://doi.org/10.1029/2009JD012773, 2010.

Pruppacher, H. and Klett, J.: Microphysics of Clouds and Precipitation, Springer, Dordrecht, Netherlands, ISBN 9780792342113, 2010.

Ratcliffe, N. G., Ryder, C. L., Bellouin, N., Woodward, S., Jones, A., Johnson, B., Wieland, L.-M., Dollner, M., Gasteiger, J., and Weinzierl, B.: Long-range transport of coarse mineral dust: an evaluation of the Met Office Unified Model against aircraft observations, Atmos. Chem. Phys., 24, 12161–12181, https://doi.org/10.5194/acp-24-12161-2024, 2024.

Renard, J.-B., Dulac, F., Durand, P., Bourgeois, Q., Denjean, C., Vignelles, D., Couté, B., Jeannot, M., Verdier, N., and Mallet, M.: In situ measurements of desert dust particles above the western Mediterranean Sea with the balloon-borne Light Optical Aerosol Counter/sizer (LOAC) during the ChArMEx campaign of summer 2013, Atmos. Chem. Phys., 18, 3677–3699, https://doi.org/10.5194/acp-18-3677-2018, 2018.

Rodakoviski, R., Kok, J., and Chamecki, M.: Dust Settling From Turbulent Layers in the Free Troposphere: Implications for the Saharan Air Layer, J. Geophys. Res.-Atmos., 128, https://doi.org/10.1029/2022JD037724, 2023.

Rosenberg, P. D., Parker, D. J., Ryder, C. L., Marsham, J. H., Garcia-Carreras, L., Dorsey, J. R., Brooks, I. M., Dean, A. R., Crosier, J., McQuaid, J. B., and Washington, R.: Quantifying particle size and turbulent scale dependence of dust flux in the Sahara using aircraft measurements, J. Geophys. Res.-Atmos., 119, 7577–7598, https://doi.org/10.1002/2013JD021255, 2014.

Ryder, C. L., Highwood, E. J., Lai, T. M., Sodemann, H., and Marsham, J. H.: Impact of atmospheric transport on the evolution of microphysical and optical properties of Saharan dust, Geophys. Res. Lett., 40, 2433–2438, https://doi.org/10.1002/grl.50482, 2013a.

Ryder, C. L., Highwood, E. J., Rosenberg, P. D., Trembath, J., Brooke, J. K., Bart, M., Dean, A., Crosier, J., Dorsey, J., Brindley, H., Banks, J., Marsham, J. H., McQuaid, J. B., Sodemann, H.,

and Washington, R.: Optical properties of Saharan dust aerosol and contribution from the coarse mode as measured during the Fennec 2011 aircraft campaign, Atmos. Chem. Phys., 13, 303–325, https://doi.org/10.5194/acp-13-303-2013, 2013b.

Ryder, C. L., Marenco, F., Brooke, J. K., Estelles, V., Cotton, R., Formenti, P., McQuaid, J. B., Price, H. C., Liu, D., Ausset, P., Rosenberg, P. D., Taylor, J. W., Choularton, T., Bower, K., Coe, H., Gallagher, M., Crosier, J., Lloyd, G., Highwood, E. J., and Murray, B. J.: Coarse-mode mineral dust size distributions, composition and optical properties from AER-D aircraft measurements over the tropical eastern Atlantic, Atmos. Chem. Phys., 18, 17225–17257, https://doi.org/10.5194/acp-18-17225-2018, 2018.

Ryder, C. L., Highwood, E. J., Walser, A., Seibert, P., Philipp, A., and Weinzierl, B.: Coarse and giant particles are ubiquitous in Saharan dust export regions and are radiatively significant over the Sahara, Atmos. Chem. Phys., 19, 15353–15376, https://doi.org/10.5194/acp-19-15353-2019, 2019.

Savvakis, V., Schön, M., Nicoll, K. A., Ryder, C. L., Papetta, A., Kezoudi, M., Marenco, F., Bange, J., and Platis, A.: In-situ observations of charged Saharan dust from an uncrewed aircraft system, Aerosol Sci. Tech., 58, 1249–1266, https://doi.org/10.1080/02786826.2024.2372399, 2024.

Saxby, J., Beckett, F., Cashman, K., Rust, A., and Tennant, E.: The impact of particle shape on fall velocity: Implications for volcanic ash dispersion modelling, J. Volcanol. Geoth. Res., 362, 32–48, https://doi.org/10.1016/J.JVOLGEORES.2018.08.006, 2018.

Seinfeld, J. H. and Pandis, S. N.: Atmospheric Chemistry and Physics : From Air Pollution to Climate Change, New York: John Wiley & Sons, Inc., ISBN 978-1-118-94740-1, 2016.

Shao, Y., Wyrwoll, K.-H., Chappell, A., Huang, J., Lin, Z., McTainsh, G. H., Mikami, M., Tanaka, T. Y., Wang, X., and Yoon, S.: Dust cycle: An emerging core theme in Earth system science, Aeolian Res., 2, 181–204, https://doi.org/10.1016/j.aeolia.2011.02.001, 2011.

Tegen, I. and Lacis, A. A.: Modeling of particle size distribution and its influence on the radiative properties of mineral dust aerosol, J. Geophys. Res.-Atmos., 101, 19237–19244, https://doi.org/10.1029/95JD03610, 1996.

Toth III, J. R., Rajupet, S., Squire, H., Volbers, B., Zhou, J., Xie, L., Sankaran, R. M., and Lacks, D. J.: Electrostatic forces alter particle size distributions in atmospheric dust, Atmos. Chem. Phys., 20, 3181–3190, https://doi.org/10.5194/acp-20-3181-2020, 2020.

Ulanowski, Z., Bailey, J., Lucas, P. W., Hough, J. H., and Hirst, E.: Alignment of atmospheric mineral dust due to electric field, Atmos. Chem. Phys., 7, 6161–6173, https://doi.org/10.5194/acp-7-6161-2007, 2007.

van der Does, M., Korte, L. F., Munday, C. I., Brummer, G.-J. A., and Stuut, J.-B. W.: Particle size traces modern Saharan dust transport and deposition across the equatorial North Atlantic, Atmos. Chem. Phys., 16, 13697–13710, https://doi.org/10.5194/acp-16-13697-2016, 2016.

van der Does, M., Knippertz, P., Zschenderlein, P., Harrison, R. G., and Stuut, J. B. W.: The mysterious long-range transport of giant mineral dust particles, Sci. Adv., 4, https://doi.org/10.1126/sciadv.aau2768, 2018.

Varga, G., Dagsson-Waldhauserová, P., Gresina, F., and Helgadottir, A.: Saharan dust and giant quartz particle transport towards Iceland, Sci. Rep., 11, 1–12, https://doi.org/10.1038/s41598-021-91481-z, 2021.

Volken, M. and Schumann, T.: A Critical review of below-cloud aerosol scavenging results on Mt. Rigi, Water Air Soil Poll., 68, 15–28, https://doi.org/10.1007/BF00479390, 1993.

Walters, D., Baran, A. J., Boutle, I., Brooks, M., Earnshaw, P., Edwards, J., Furtado, K., Hill, P., Lock, A., Manners, J., Morcrette, C., Mulcahy, J., Sanchez, C., Smith, C., Stratton, R., Tennant, W., Tomassini, L., Van Weverberg, K., Vosper, S., Willett, M., Browse, J., Bushell, A., Carslaw, K., Dalvi, M., Essery, R., Gedney, N., Hardiman, S., Johnson, B., Johnson, C., Jones, A., Jones, C., Mann, G., Milton, S., Rumbold, H., Sellar, A., Ujiie, M., Whitall, M., Williams, K., and Zerroukat, M.: The Met Office Unified Model Global Atmosphere 7.0/7.1 and JULES Global Land 7.0 configurations, Geosci. Model Dev., 12, 1909–1963, https://doi.org/10.5194/gmd-12-1909-2019, 2019.

Weinzierl, B., Petzold, A., Esselborn, M., Wirth, M., Rasp, K., Kandler, K., Schütz, L., Koepke, P., and Fiebig, M.: Airborne measurements of dust layer properties, particle size distribution and mixing state of Saharan dust during SAMUM 2006, Tellus B, 61, 96–117, https://doi.org/10.1111/j.1600-0889.2008.00392.x, 2009.

Weinzierl, B., Ansmann, A., Prospero, J. M., Althausen, D., Benker, N., Chouza, F., Dollner, M., Farrell, D., Fomba, W. K., Freudenthaler, V., Gasteiger, J., Groß, S., Haarig, M., Heinold, B., Kandler, K., Kristensen, T. B., Mayol-Bracero, O. L., Müller, T., Reitebuch, O., Sauer, D., Schäfler, A., Schepanski, K., Spanu, A., Tegen, I., Toledano, C., and Walser, A.: The Saharan aerosol long-range transport and aerosol-cloud-interaction experiment: Overview and selected highlights, B. Am. Meteorol. Soc., 98, 1427–1451, https://doi.org/10.1175/BAMS-D-15-00142.1, 2017.

Woodward, S.: Modelling the atmospheric life cycle and radiative impact of mineral dust in the Hadley Centre climate model, J. Geophys. Res., 106, 18155–18166, https://doi.org/10.1029/2000JD900795, 2001.

Woodward, S., Sellar, A. A., Tang, Y., Stringer, M., Yool, A., Robertson, E., and Wiltshire, A.: The simulation of mineral dust in the United Kingdom Earth System Model UKESM1, Atmos. Chem. Phys., 22, 14503–14528, https://doi.org/10.5194/acp-22-14503-2022, 2022.

Xu, C., Ma, Y., Yang, K., and You, C.: Tibetan Plateau Impacts on Global Dust Transport in the Upper Troposphere, J. Climate, 31, https://doi.org/10.1175/JCLI-D-17-0313.1, 2018.

Yang, W., Marshak, A., Kostinski, A. B., and Várnai, T.: Shape-induced gravitational sorting of Saharan dust during transatlantic voyage: Evidence from CALIOP lidar depolarization measurements, Geophys. Res. Lett., 40, 3281–3286, https://doi.org/10.1002/grl.50603, 2013.

Zender, C. S., Bian, H., and Newman, D.: Mineral Dust Entrainment and Deposition (DEAD) model: Description and 1990s dust climatology, J. Geophys. Res.-Atmos., 108, https://doi.org/10.1029/2002jd002775, 2003.

Zhao, A., Ryder, C. L., and Wilcox, L. J.: How well do the CMIP6 models simulate dust aerosols?, Atmos. Chem. Phys., 22, 2095–2119, https://doi.org/10.5194/acp-22-2095-2022, 2022.